

Balu Puthoor Bhasi

# Study on the influence of entrapped air in a suction anchor during installation

Master's thesis in Msc. Naval architecture

Supervisor: Prof. Henry Peter Piehl

Co-supervisor: Prof. Vilmar Æsøy

June 2023



Balu Puthoor Bhasi

# **Study on the influence of entrapped air in a suction anchor during installation**

Master's thesis in Msc. Naval architecture  
Supervisor: Prof. Henry Peter Piehl  
Co-supervisor: Prof. Vilmar Æsøy  
June 2023

Norwegian University of Science and Technology  
Faculty of Engineering  
Department of Ocean Operations and Civil Engineering





# Preface

This thesis documents research conducted from January to May 2023 at the Norwegian University of Science and Technology in NTNU Ålesund, Department of Ocean Operations and Civil Engineering, Faculty of Engineering. The thesis study was carried out to earn a Master of Science degree in Naval Architecture. Undertaking this research provided an opportunity to challenge myself and acquire new skills outside my comfort zone.

Throughout the study, I learned how to approach engineering problems systematically and design an experimental setup. I also gained knowledge about sensors, micro-controllers, and their integration into an experimental setups, which was previously unfamiliar to me. It was fascinating to observe the connection between experimental results and mathematical models. Additionally, I further developed my programming skills.

I would like to express my gratitude to my supervisor, Prof. Henry Piehl, for guiding me throughout the study and providing valuable insights. Despite my occasional foolish questions, he patiently supported me, pointed out challenges, and provided constructive criticism, which greatly contributed to my growth and learning. I also appreciate the contributions of my co-supervisor, Prof. Vilmar Æsøy, who assisted in the development of the test setup and offered solutions to various challenges. I extend my thanks to the research lab assistants at NTNU Ålesund for providing the necessary facilities for conducting the tests.

I am thankful to Entail AS, particularly Stefan, Pål, and Martin, for their assistance in the thesis work and providing industrial data.

Finally, I am deeply grateful to my family (Mom, Dad, Sister, and brother-in-law) and friends, especially Rahul, Pranav and Suhas, for their unwavering support during both the highs and lows of this journey.

Balu Puthoor Bhasi  
Msc.Naval Architecture  
NTNU Ålesund  
June 7, 2023

# Abstract

In the past few years suction anchors have been increasingly used as a foundation for different sub-sea installations and for mooring of different floating structures. A typical suction anchor is a hollow steel cylinder with a closed top which uses under pressure to penetrate into the seabed. The top plate comes with a vent valve to offer ventilation during lowering and installation. The installation of suction anchor requires examination and control of dynamic loads and displacements. When a suction anchor is lowered through the splash zone, insufficient air ventilation through the vent valve will create an upward force which might cause the lifting wire to become slack. This can result in snap forces on the lifting wire when struck by a wave the next moment. Many of the suction anchors have been installed using simplified rules and models. But these models do not capture the entrapped air effect. A suction anchor analysis tries to maximize the achievable weather windows by assessing the hydrodynamic forces and many people are doing so using these simple models. But most people are excluding the entrapped air effect. Therefore, it is important to investigate it.

This master thesis presents an investigation on the entrapped air effect as well as hydrodynamic effects and loads acting on a suction anchor during installation through scaled down experiments and numerical analysis. An experimental setup consisting of several electronic sensors, micro controllers and mechanical devices was designed and developed to measure different parameters that determine the behavior of suction anchor while lowering. The experimental setup facilitated for an integrated and synchronous recording of sensor data which provides the force, pressure and displacement information throughout the lowering process.

The total lowering process was decomposed into different test cases that isolate each physical effect. Scaled down experiments were conducted for each test case and the measurement data was recorded. Simultaneously, a mathematical model which is an ordinary differential equation (ODE) was formulated for the lowering process and simulated using time integration method. The experimental results were used to validate the mathematical model developed. Comparing the simulation results with the experiment data, it was observed that the experimental results had a good match with the mathematical model results for static test cases. For dynamic cases, some mismatches were observed in the pressure and force data during the transient phase. The mathematical model used approximation to calculate the hydrodynamic forces and the pressure drop due to air ventilation was calculated using orifice flow equation. The possible reason for the mismatch could be that the mathematical model failed to capture the ventilation effect or there might be some other effects that occur during lowering which were not accounted in the mathematical model. This was observed in the late stage of the thesis work and error correction has not been achieved. The mathematical model should be extended or repeated experiments have to be con-

ducted to better capture the dynamic effects in the transient phases.

Finally, in order to investigate the potential improvement of the suction anchor lowering process, a parametric study for different lowering velocity and vent hole size was performed using the developed experimental setup. The results were used to analyze the influence of each parameter on the behavior of suction anchor and recommendations to improve the lowering operation were discussed.

## Thesis Agreement

### Study on the influence of entrapped air in a suction anchor during installation

#### Background

Suction anchors are becoming more and more popular with the rise of floating Oil& Gas and floating wind solutions. Control of the motion and forces acting on a suction anchor during installation is crucial to ensure safety of the operation. Suction anchors are hollow steel cylinders with closed top which have a vent valve opening on the top plate to offer ventilation during different phases of installation. Insufficient ventilation of air during the lowering of suction anchor into water can result in an upward force due to trapped air that may cause potential slack in the lifting wire. This may lead to snap forces in the lifting wire when struck by a wave. Many of the suction anchor have been installed using simplified rules and simple methods. But these methods does not capture the effect of entrapped air correctly. Therefore it is important to study it.

#### Objective and Research questions

The primary objective of the thesis is to investigate on the entrapped air effect as well as hydrodynamic effects and loads acting on a suction anchor during installation. In order to achieve the objective, scaled down experiments and numerical analysis of the lowering process is performed. The experimental measurements are used to validate the results of numerical model developed. Additionally, the study seeks to discuss measures for potential improvement of the lowering process. The research questions for this master thesis are as follows:.

1. How to conduct the experimental study on the entrapped air effect and hydrodynamic effects during suction anchor lowering?
2. How to analyse the lowering process numerically and validate it ?
3. Discuss ways to improve the suction anchor lowering process.

#### Scope and limitations

The scope of this thesis is within the boundary of experimental study of the suction anchor lowering operation and analytical modelling of the physics involved that focus on the entrapped air effect. The experimental results will be limited to scaled down experiments in the towing tank at NTNU Ålesund. Scaled down experiments were chosen because full scale experiments are expensive and a model test is thought to be more effective at capturing the physical effects that occur in the real world because it contains all of the laws of physics. One of the limitations of this thesis is that it does not take into account the wave effects during lowering of the suction anchor. The waves bring oscillating piston movement of air column inside the suction anchor. Due to technical limitations, the experiment is carried out only in still water with focus on only the heave motion.

#### Student:

Mr. Balu Puthoor Bhasi  
Msc Naval Architecture  
NTNU Ålesund

#### Supervisor:

Prof. Henry Peter Piehl

#### Co-Supervisor:

Prof. Vilmar Æsøy



# Contents

<b>1</b>	<b>Introduction</b>	<b>9</b>
1.1	Background and Motivation . . . . .	9
1.2	Problem Definition . . . . .	11
1.3	Objective and Research Questions . . . . .	14
1.4	Scope and Limitations . . . . .	14
<b>2</b>	<b>Literature Review</b>	<b>15</b>
2.1	Related works . . . . .	15
2.2	Basic Theory . . . . .	16
2.2.1	Equation of State . . . . .	16
2.2.2	Bernoulli's Theorem . . . . .	17
2.2.3	Continuity Equation . . . . .	17
2.2.4	Flow Through Orifice . . . . .	17
<b>3</b>	<b>Methods</b>	<b>18</b>
3.1	Analytical Modelling . . . . .	18
3.1.1	Concept model . . . . .	19
3.1.2	Assumptions . . . . .	20
3.1.3	Air pressure Modelling . . . . .	20
3.1.4	Air Ventilation . . . . .	23
3.1.5	Wire stiffness force . . . . .	25
3.1.6	Added mass and Damping force . . . . .	25
3.1.7	Slamming Force . . . . .	26
3.1.8	Simulation model . . . . .	27
3.2	Experimental Method . . . . .	29
3.2.1	Existing setup / Facilities . . . . .	29
3.2.2	Experimental test setup development . . . . .	29
3.2.3	Sensor devices . . . . .	31
3.2.4	Design and build test specimen . . . . .	33
3.2.5	Experiment Plan . . . . .	34
<b>4</b>	<b>Results and Comparison</b>	<b>40</b>
4.1	Validation of simulation model . . . . .	40
4.2	Parametric study . . . . .	43
4.2.1	Changing lowering velocity . . . . .	43
4.2.2	Changing Vent valve size . . . . .	44

<b>5 Discussion and Conclusion</b>	<b>46</b>
<b>6 Future Works</b>	<b>49</b>
<b>A Simulation Code</b>	<b>51</b>

# List of Figures

1.1	Suction anchor applications . . . . .	10
1.2	Suction anchor lowering source - <a href="http://www.neodrill.com">www.neodrill.com</a> . . . . .	10
1.3	Sub-sea lifting phases . . . . .	11
1.4	Schematic diagram - suction anchor lifting . . . . .	12
1.5	Air ventilation during suction anchor lowering source- <a href="http://www.neodrill.com">www.neodrill.com</a> . . . . .	13
3.1	Concept model . . . . .	20
3.2	Lowering process schematic diagram . . . . .	21
3.3	Pressure drop during fluid flow through orifice source - [7] . . . . .	23
3.4	Approximate added mass of a semi submerged vertical cylinder source- [7] . . . . .	26
3.5	Wet closed Simulation results . . . . .	28
3.6	Experimental Setup - Initial Concept . . . . .	29
3.7	Final Experimental Setup . . . . .	30
3.8	Sensor measurement setup - Principle concept . . . . .	30
3.9	Multi-sensor measurement circuit setup . . . . .	31
3.10	HX710B pressure sensor module source- <a href="http://www.electroschematics.com">www.electroschematics.com</a> [3] . . . . .	31
3.11	Pressure sensor calibration . . . . .	32
3.12	Force sensor source- <a href="http://www.hbm.com">www.hbm.com</a> [5] . . . . .	32
3.13	Rotation sensor AS5600 source - <a href="http://www.ams.com">www.ams.com</a> [4] . . . . .	33
3.14	Rotation sensor setup . . . . .	33
3.15	Test specimen . . . . .	34
3.16	Experiment Plan . . . . .	34
3.17	Force sensor sensor calibration . . . . .	35
3.18	Dynamic dry - Position plot . . . . .	36
3.19	Dynamic dry - Force plot . . . . .	36
3.20	Fourier analysis - position data . . . . .	36
3.21	Wet closed static - Depth measurement . . . . .	37
3.22	Wet closed static - Pressure measurement . . . . .	38
3.23	Wet closed dynamic . . . . .	38
3.24	Wet open dynamic . . . . .	39
4.1	Simulation model validation - Static water depth . . . . .	40
4.2	Simulation model validation - Static pressure . . . . .	41
4.3	Wet closed dynamic . . . . .	42
4.4	Wet open dynamic . . . . .	43
4.5	Varying lowering velocity for constant hole size . . . . .	44
4.6	Velocity comparison for different vent valve size . . . . .	45

4.7 Varying vent valve size . . . . . 45

## List of Tables

2.1 Assumed parameters of the ambient air phase . . . . . 16

3.1 Model parameters . . . . . 21

3.2 Principle dimension . . . . . 34

# Chapter 1

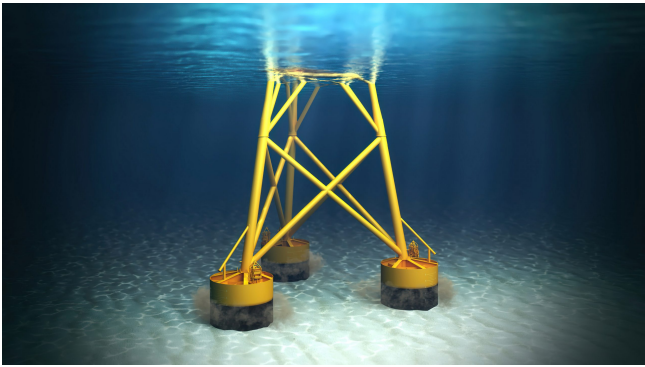
## Introduction

The oil and gas industry have been important from past years due to the growing energy demand. This has led to an increased pressure on the oil and gas corporation which forced them to discover resources in more difficult deep water conditions. As a result, the design and installation of offshore facilities are becoming more challenging. In the field of offshore installation, suction anchors are becoming the preferred foundation solution for mooring different types of floating structures and sub-sea installations. They have been proven very adaptable, effective, and environment friendly. Suction anchor lifting and installation is a common marine operation in such offshore installation projects. Inadequate safety while performing these operation can have disastrous results in terms of loss of life, damage to the environment, and destruction of assets. Planning of such marine operations encompasses crucial tasks required to guarantee a system that is safe, effective, and environment friendly.

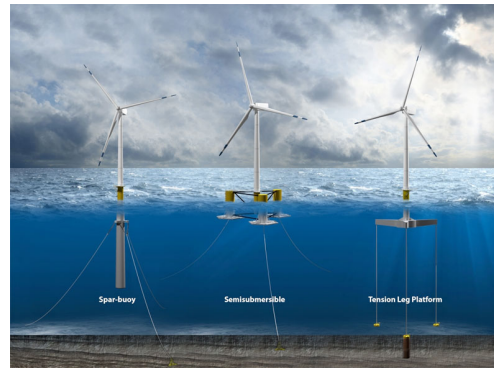
### 1.1 Background and Motivation

A Marine Operation is a non-routine operation of a limited duration related to handling of object(s) and/or vessel(s) in the marine environment. These operations are essential to the global economy, as they allow for the extraction and transportation of goods and natural resources across the world. One of the most important aspects of marine operations is ensuring the safety of the vessels and personnel involved. This involves the use of advanced technology and strict regulations to prevent accidents and protect the environment.

The need for marine operations and installations are increasing as the oil and gas sector develops. This prompted the industry to adopt more difficult deep-water sub-sea resource extraction techniques. Suction anchors are frequently used for both the long-term mooring of floating production and storage vessels as well as the foundation of sub-sea structures. For the purpose of supporting offshore wind farms and jacket platforms, suction anchors typically replace piling. Figure 1.1 illustrates some of the applications of suction anchor in various offshore projects.



(a) Substructure for jackets  
source- [www.ocean-energyresources.com](http://www.ocean-energyresources.com)



(b) Mooring of semisub and floating wind  
source- [www.acteon.com](http://www.acteon.com)

Figure 1.1: Suction anchor applications

Suction anchors mainly come in the form of hollow steel cylinders with closed top. They are secured into the seabed by creating a under pressure by pumping out water from within. In order to offer ventilation during lowering, landing, and soil penetration as well as to evacuate air during lowering through splash zone, one or more vent valves are provided on the top plate. As soon as the self-weight penetration has been completed, these valves must be closed so that an under pressure can be created inside to facilitate leveling and final penetration. In most cases, the vertical side walls are solid. To prevent soil fracture during landing and penetration, perforations are seen to be incorporated into the lower portion of walls. The diameter to height ratio of a suction anchor can vary from 0.3 to 1.25, depending on usage and soil conditions. Figure1.2 shows a typical suction anchor.



Figure 1.2: Suction anchor lowering  
source - [www.neodrill.com](http://www.neodrill.com)

During installation, the suction anchor may be subjected to significant hydrodynamic forces. The design of a suction anchor should be based on a thorough study to guarantee that it can sustain the necessary forces during installation, leveling, and lowering, as well as include a safety margin. The installation process of the suction anchor requires examination and management of the dynamic loads and displacement. During lifting and lowering, the displacements and forces acting on the anchor are substantial, and it is crucial to ensure that they are kept under control.

The main focus is given to the tension developed in the lifting line during the installation. It is important to assess the most critical loads that could be imposed on the suction anchor and the lifting equipment during a lifting operation at a given sea state. Contractors, class societies, and organizations that carry out third-party verification work utilize conservative calculation methods in order to be on the safe side.

Dynamic forces in marine operations seem to traditionally rely more on experience than exact calculations. This knowledge is still an essential part of planning and carrying out marine operations. Dynamic forces on sub-sea structures are difficult to estimate because of their complex geometries. The numerical model software solutions that have been created to handle this complex procedure do not take into account some physical aspects that occur in real life. In order to improve physical insights and computational approaches, it is therefore necessary to look for uncertainties in these numerical models. The challenges that engineers now have in regulating a suction anchor's motions during installation served as the motivation for this thesis. Scaled down experiments will replicate the physical characteristics of the actual operation and also captures the dynamic forces accurately.

## 1.2 Problem Definition

A suction anchor deployment operation can be broken down in to many phases. DNV recommended practice [1] identifies the following stages as the main phases of a sub-sea lifting operation.

- Lift off
- Splash zone crossing
- Lowering to seabed
- Vessel reposition and landing on seabed

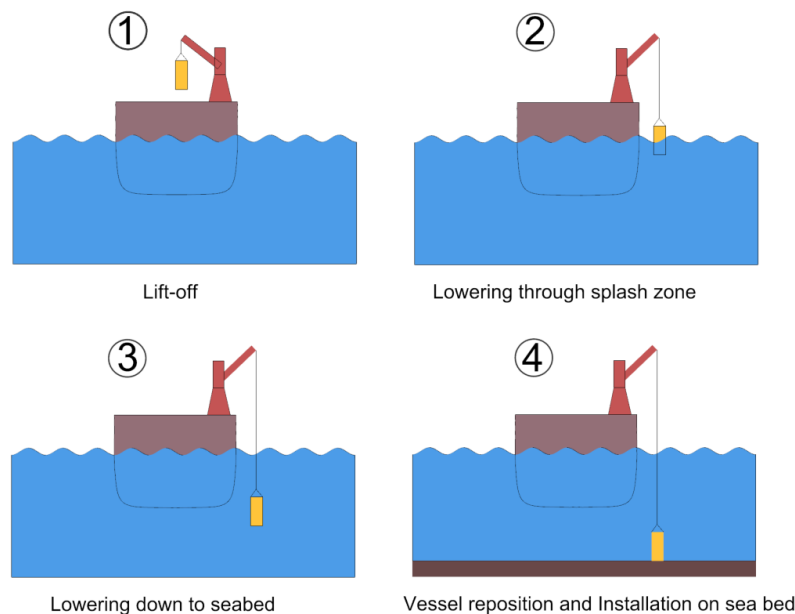


Figure 1.3: Sub-sea lifting phases

The suction anchor is lifted off from the vessel's deck and then shifted horizontally from its deck location to the lowering position. It is then lowered through the splash zone, where it is subjected to large wave forces. The crane pays out until the suction anchor is just above the seabed. The vessel is then re-positioned before the anchor is placed on the seafloor to ensure that it is landed on its deployment location. Prior to offshore execution, engineering is performed on each of the aforementioned phases to ensure a reasonable possibility of a successful operation. Figure 1.3 shows an illustration of different phases of lifting a suction anchor.

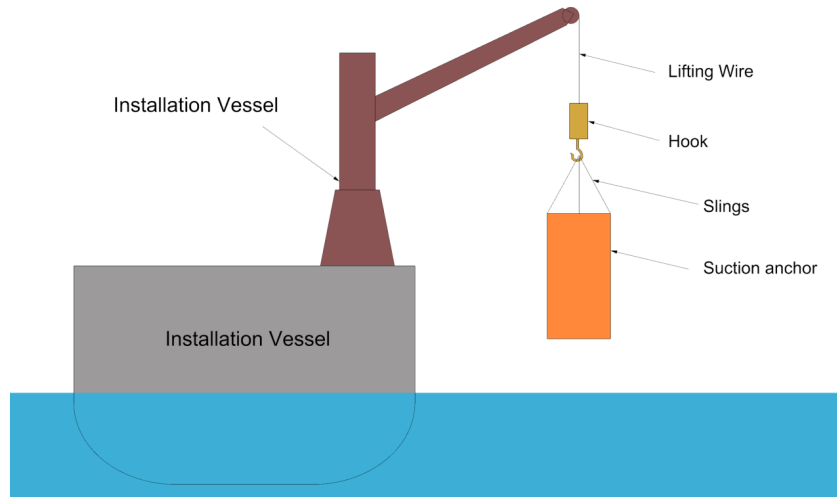


Figure 1.4: Schematic diagram - suction anchor lifting

Figure 1.4 shows a schematic diagram of a suction anchor lifting setup. Due to hydrodynamic induced motions and loads, significant forces are experienced during the splash zone lowering phase, causing the lifting line and slings to be subjected to potential slack. Therefore this phase is given much attention when determining the design sea state for installation. The design sea state is optimized using hydrodynamic analyses such as time-domain simulations, computational fluid dynamics, and model testing. However each of these methods have their own limitations in addition to being time consuming and costly for model testing. To fully represent the physical phenomena that occurs in the real world, it is necessary to look for uncertainties in the aforementioned computational methods. A model test is thought to be more effective in capturing the physical effects that occur in the real world because it contains all of the laws of physics. The model test results are then scaled to find the behaviour in full scale. The scaling of the results can be made using either Reynolds number or Froude number. Reynolds scaling will be suitable for fluid flow where viscous effects are dominant. Whereas for flows where gravity effects are dominant Froude scaling can be a relevant approach. The principal source of rules and standards for sub-sea lifting operations is DNV-RP-H103 [1]. They have developed some standards and recommendation which guarantee that marine operations are planned and executed in accordance with accepted safety standards. The document specifies guidelines for each phases of sub-sea lifting operation. For estimating the hydrodynamic forces acting on a sub-sea structure when it is lowered into the splash zone, DNV suggests a simplified method to have a conservative estimate of significant forces that arise during the installation in an early planning stage. The loads computed using this method can be used as design criteria by design firms without comprehensive hydrodynamic analysis. The method assumes that the lifted object is small compared to the wavelength. Also, the method does not take in to account the slack in the slings, which makes it not well suited



for suction anchor lifting. These limitations might result in too conservative estimates of the design sea state, which would increase installation cost and necessitate the use of bigger installation vessels and more restrictive weather windows.

The method for calculating added mass, damping, and impact forces on the suction anchor when lowered through the splash zone is well described by the simplified approach. It is also advised in the document that slack in the lifting wire should be avoided as far as possible to eliminate snap forces. Furthermore, the simplified method does not differentiate between the slings and the lifting wire. To overcome this limitation time-domain analysis is performed, which has the advantage that it include slings and that we can allow slings to go slack even though the lifting wire is not slack. Insufficient air ventilation in suction anchors during lowering through the splash zone can create upward force from trapped air, resulting in slack of lifting wire and slings when exceeded beyond a limit. However, the simplified method does not take into account this entrapped air effect as per section 4.3.5.3 of DNV-RP-H103[1]. It is important to ensure adequate air ventilation to prevent this issue. To ensure proper air evacuation, a vent hole is present on the top plate of suction anchors. A small ventilation hole can cause substantial pressure force and potentially tilt the anchor, rendering the lifting wire slack. The ratio of the suction anchor diameter to the vent hole diameter must be carefully calculated to prevent such occurrence. Figure 1.5 shows the air ventilation effect in a suction during splash zone crossing. Potential solvers does not account this entrapped air effect. However, advanced tools like Computation Fluid Dynamics (CFD) can be utilised to estimate the forces during the lifting. But CFD is computationally expensive and time consuming and also they may fail to capture all the physical effects that occur during the lowering due to error in modelling or simulation setup.



*Figure 1.5: Air ventilation during suction anchor lowering  
source- [www.neodrill.com](http://www.neodrill.com)*

### 1.3 Objective and Research Questions

The primary objective of the thesis is to investigate the entrapped air effect as well as hydrodynamic effects and loads acting on a suction anchor during installation. In order to achieve the objective, scaled down experiments and numerical analysis of the lowering process will be performed. The experimental measurements will be used to validate the results of numerical analysis. Additionally, the study seeks to discuss measures for potential improvement of the lowering process.

The research questions are the goals for this master thesis and the report focuses to answer or discuss it. They are as follows:

1. How to conduct the experimental study on the entrapped air effect and hydrodynamic effects during suction anchor lowering?
2. How to analyse the lowering process numerically and validate it ?
3. Discuss ways to improve the suction anchor lowering process.

### 1.4 Scope and Limitations

The scope of this thesis is within the boundaries of experimental study of the suction anchor lowering operation and analytical modelling of the physics involved that focus on the entrapped air effect. The experimental results will be limited to scaled down experiments in the towing tank at NTNU Alesund. The scaled down experiments were chosen due to high expense for conducting full scale experiments and a CFD analysis can be computationally expensive and time consuming. However, at times CFD analysis may fail to represent the actual lowering process due to possible errors in modelling simulation setup. Therefore model scale experiments were considered more accurate since it has all the physics included. All assumptions and conclusions are checked with the mathematical model and/or references to physical effects in a logical manner.

One of the limitations of this thesis is that it does not take into account the wave effects during lowering of the suction anchor. The waves bring oscillating piston movement of air column inside the suction anchor. Due to technical limitations, the experiment is carried out only in still water with focus on only the vertical motion.

# Chapter 2

## Literature Review

### 2.1 Related works

One of the main source of marine lifting operation regulations and standards is DNV-RP-H103 [1]. They have produced a standard which is intended to ensure that marine operations are designed and performed in accordance with recognized safety levels and to describe “current industry good practice”. This recommended practice gives guidance for lifting operations through the splash zone and lowering of objects down to the seabed. The objective of the “lifting through wave zone” part of the document is to improve modelling and analysis methods to obtain more accurate prediction of design loads.

The document also provides a simplified method to have a simple conservative estimate of the hydrodynamic forces acting during lifting. According to DNV-RP-H103[1], the hydrodynamic forces acting on a body when lowering through a water surface is a time dependent function of impact force, varying buoyancy force, hydrodynamic mass force and drag force. The simplified method calculates characteristic total force as:

$$F_{total} = F_{static} + F_{hyd} \quad (2.1)$$

where  $F_{static}$  is the static weight of the object and  $F_{hyd}$  is the hydrodynamic forces acting on the object when it is lowered through water surface. The hydrodynamic force is calculated using the equation:

$$F_{hyd} = \sqrt{(F_D + F_{slam})^2 + (F_M - F_p)^2} \quad (2.2)$$

where  $F_D$  is the hydrodynamic drag force,  $F_{slam}$  is the impact or slamming force,  $F_M$  is the added mass force and  $F_p$  is the varying buoyancy force. The document also specifies a slack sling criterion to avoid snap forces in the lifting wire. The snap forces in slings or lifting wire may occur if the hydrodynamic force exceeds the static weight of the object. The slack sling criterion to avoid snap loads is as follows:

$$F_{hyd} \leq 0.9F_{static} \quad (2.3)$$

When a suction anchor is lowered, insufficient ventilation can create upward force that causes the lifting wire and slings to go slack. But the simplified method does not take into account this effect that can make the slack sling criterion to fail (see equation 2.2). Therefore the simplified method will be less suitable for the analysis of suction anchors. A lot of published works are available for

modeling and analysis of marine operations, covering different aspects of the operation. Sound knowledge is important to be able to simulate real-life events as accurately as needed. Knowledge is also the key to determine system boundaries and to make reasonable assumptions and simplifications.

Hydrodynamic coefficients in heave for suction anchors with various top plate perforation levels and Diameter to Height (D/H) ratio are discussed in the research paper published by Frøydis Sollaas and Peter Christian [6]. The motion decay technique is the test method used to evaluate the hydrodynamic coefficients for the suction anchors that are provided. The research paper includes performing a number of tests utilizing a suction anchor model with different hatch openings. For suction anchors with perforations in the top plate, it was discovered that the added mass decreased and the damping increased with increasing perforation levels. A suction anchor analysis tries to maximise the achievable weather windows by assessing the hydrodynamic forces and many people are doing so, but most people are excluding this entrapped air effect. All of the aforementioned references use entrapped water effect in the suction anchor which is related hydrodynamic forces. There are no explanations on the effect of entrapped air that could bring potential slack in the lifting wire. Thus this study put forward a relevance to look into these aspects and the finding of this study could be beneficial to evaluate if this effect is significant enough to take into consideration.

## 2.2 Basic Theory

Before investigating practical problems, this section describes some of the basic theory and equations used to formulate the mathematical model. By utilising these equations and considering the relevant physical parameters (e.g., mass, density, cross-sectional area, hydrodynamic coefficients etc), it is possible to create a mathematical model that describes the motion of the suction anchor during the lowering process. Once the mathematical model is established, ODE solver that uses time integration method can be employed to simulate and analyze the system's behavior. These methods allow for the computation of variables like position, velocity, and pressure at different time points, providing insights into the dynamics of the suction anchor lowering process and the entrapped air effect.

### 2.2.1 Equation of State

If the formation of entrapped air pockets is assumed to be relevant, the description of the flow dynamics in the compressible air phase requires at least one basic equation. The equation of state of an ideal gas which is given by:

$$pV = nRT \quad (2.4)$$

where  $r$  is the specific gas constant,  $v$  is the volume,  $n$  mass in moles of gas and  $t$  is the temperature of the air. The assumed conditions for ambient air phase are summarised in the Table 2.1.

Temperature	$T$	15deg
Pressure	$P_e$	101325 $P_a$
Specific gas constant	$R$	287.058 $\frac{J}{kg.K}$

Table 2.1: Assumed parameters of the ambient air phase

For an isothermal process of a compressible ideal gas, the relation between the pressure and volume can be described as follows:

$$pV = RT = \text{constant}$$

### 2.2.2 Bernoulli's Theorem

The fluid flow for water and air is described by the Bernoulli equation, which can be obtained from the integration of the Euler equation along a streamline by applying conservation of linear momentum. In addition, an equation of state is required for describing the pressure density relation of the compressible air phase. Bernoulli's principle states that for an inviscid and stationary fluid flow, the overall energy composed of the pressure head, kinetic and potential energy stays constant along a streamline. It is expressed by the following equation:

$$P + \frac{1}{2}\rho u^2 + \rho gz = \text{const} \quad (2.5)$$

where  $p$  is the fluid pressure,  $\rho$  the fluid density,  $g$  the gravitational constant,  $u$  the fluid velocity and  $z$  the level height.

### 2.2.3 Continuity Equation

The continuity equation for in-compressible flow is a fundamental principle in fluid mechanics that describes the conservation of mass in a fluid system. It states that the mass flow rate remains constant along a streamline. Mathematically, the continuity equation for in-compressible flow can be expressed as:

$$A_1 V_1 = A_2 V_2$$

Where  $A_1$  and  $A_2$  are the cross sectional area at two different points in the flow and  $V_1$ ,  $V_2$  are the velocities of those corresponding points.

### 2.2.4 Flow Through Orifice

The Bernoulli's equation and the continuity equation is used to formulate the volumetric flow rate of a fluid through an orifice. Which is given by :

$$Q_v = CdA_2 \sqrt{\frac{2\Delta p}{\rho_a}} \quad (2.6)$$

Where  $Q$  is the volumetric flow rate in  $m^3/s$ ,  $Cd$  is the discharge coefficient, which represents the efficiency of the orifice,  $A$  the cross sectional area of the orifice ( $m^2$ ),  $p$  the pressure difference across the orifice(Pa) and  $\rho_a$  is the density of air in ( $kg/m^3$ )

In the equation 2.6, the discharge coefficient ( $Cd$ ) takes into account various factors that influence the flow efficiency, including the shape and size of the orifice, the smoothness of its surface, and the flow conditions. The value of  $Cd$  typically ranges between 0 and 1, with higher values indicating more efficient flow. It is important to note that this equation assumes in-compressible flow and neglects factors such as turbulence and viscous effects.

# Chapter 3

## Methods

In this chapter, the methods utilized in the present study are discussed in detail. The primary objective of the study is to investigate the entrapped air effect, and this investigation will be carried out through a combination of experiments and numerical analysis. To effectively study the entrapped air effect, it is essential to break down the entire lowering process into simplified test cases. Each test case will be evaluated both experimentally and analytically to gain a comprehensive understanding of the phenomenon.

The chapter is divided into two parts to address different aspects of the study. The first part focuses on the analytical modeling of the suction anchor lowering process. Initially, an assessment will be made regarding the likely forces that can act on the suction anchor and the parameters that need to be considered for studying the entrapped air effect. After identifying these forces and parameters, an analytical model will be developed, taking them into account. The model will be simulated using time integration method to analyze the behavior of the suction anchor during the lowering process. Once the analytical model is formulated, the next step is to validate it by comparing its simulation results with the experiments. The second part of the chapter is dedicated to the design and development of the experimental setup. Creating an appropriate experimental setup is crucial to conduct the necessary tests accurately. Once the experimental setup is completed, a test matrix is defined. This test matrix outlines the specific experiments that will be conducted to evaluate each physical effect that occurs during the lowering process. The chapter concludes by presenting the measurements for each experimental test cases conducted.

### 3.1 Analytical Modelling

This section focuses on the formulating an analytical model of the suction anchor lowering process. Initially, a concept model is developed to identify all the forces that act on the suction anchor while it is being lowered into water. Each force is carefully studied and evaluated to formulate the ordinary differential equation (ODEs) that describe the dynamics of the system. These ODEs capture the interaction between the suction anchor and the various forces acting upon it. Once the ODEs are formulated, they are simulated using time integration method. This simulation allows to predict the behaviour of the suction anchor during the lowering process and obtain numerical results. The simulation results obtained from the analytical model will be then compared with the experimental results obtained from different test matrix measurements later. This step is crucial

in validating the accuracy and reliability of the analytical model.

The validated model is then utilized to conduct a parametric study. This study involves varying different factors, such as vent size and lowering velocity, to investigate their effects on the lowering process. A systematical exploration of these parameter helps to optimize the lowering process for improved performance and efficiency.

### 3.1.1 Concept model

The different forces that acts on the suction anchor during the lowering process are listed below:

- **Gravity (Mg):** The force of gravity acts vertically downward and is responsible for the weight of the suction anchor
- **Buoyancy due to trapped air (Fp):** When the suction anchor is lowered into water, the air inside the anchor gets compressed, creating an upward buoyancy. This force increases with the submergence level when the valve is closed.
- **Pressure Drop due to Ventilation ( $\Delta p$ ):** If the valve is open, some of the compressed air escapes to the atmosphere, leading to pressure drop inside the suction anchor.
- **Buoyancy Force (Fb):** The suction anchor displaces water, and the volume of water displaced creates a buoyancy acting in the upward direction.
- **Hydrodynamic Force (Fhyd):** Once the suction anchor enters the water, it experiences hydrodynamic forces, such as added mass and drag forces. These forces are caused by the movement of the anchor through the water.
- **Slamming Force (Fs):** This is the force experienced by the anchor during its first entry into the water.
- **Wire stiffness Force (Fspring):** As the suction anchor is lowered, due to the weight of the anchor creates tension in the lifting wire that makes it get elongated to some extent. This elongation generates a restoring force known as the wire stiffness force. The effective weight of the anchor decreases due to buoyancy, so the force which has elongated the wire decreases.

A graphical illustration of the aforementioned forces is shown in Figure 3.1. It is important to consider these force to capture the exact behaviour of the suction anchor when lowered into water and controlling the forces can help prevent slack in the lifting wire and minimize the risk of snap loads. The following section will discuss these force in detail.

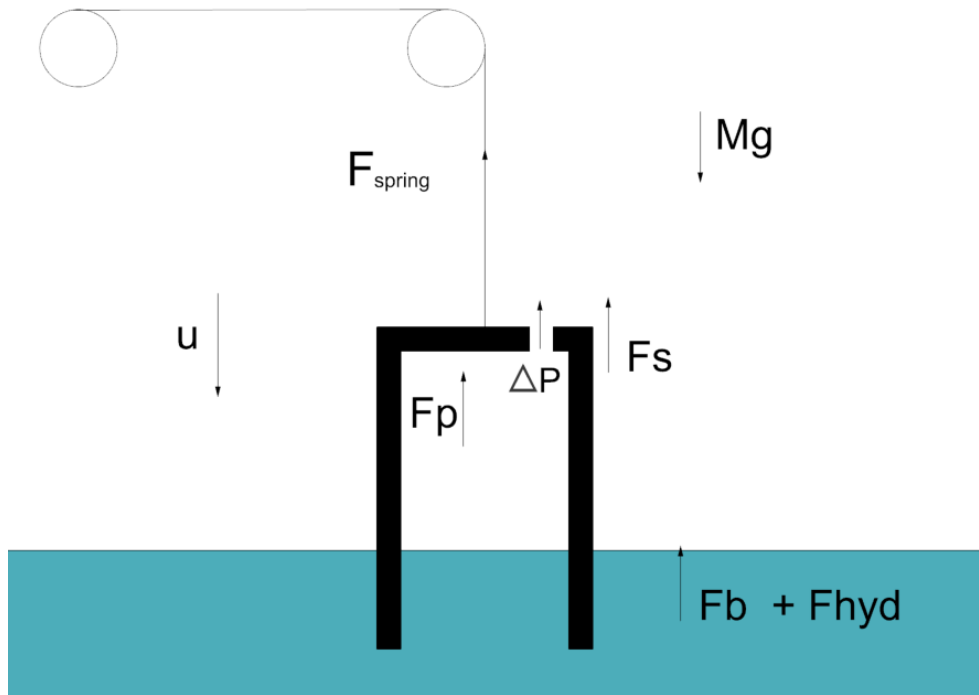


Figure 3.1: Concept model

### 3.1.2 Assumptions

The main assumptions for the analytical model is listed below.

- The water is assumed in-compressible and isothermal
- Air is considered as ideal gas
- Surface tension on the wall surface is neglected
- The experiment is assumed in still water
- The tilting of the cylinder while lowering is not considered
- The air pressure distribution inside the suction anchor is assumed uniform

### 3.1.3 Air pressure Modelling

When the suction anchor is lowered into water, it is initially filled with air. As the anchor touches the water surface, water begins to fill the anchor. In a closed valve condition, the valve prevents the escape of air from the anchor. As a consequence, the air pressure inside the suction anchor gradually increases. At the same time water exerts hydrostatic pressure on the anchor from outside. The equilibrium between the air pressure inside the suction anchor and the hydrostatic pressure at that water depth results in the variation in water level inside the anchor. Figure 3.2 shows the schematic diagram of the suction anchor in submerged condition.

The water level inside the suction anchor is denoted as 'h' and 'H' denotes the water level outside the suction anchor as shown in Figure 3.2. The pressure inside the anchor will be the



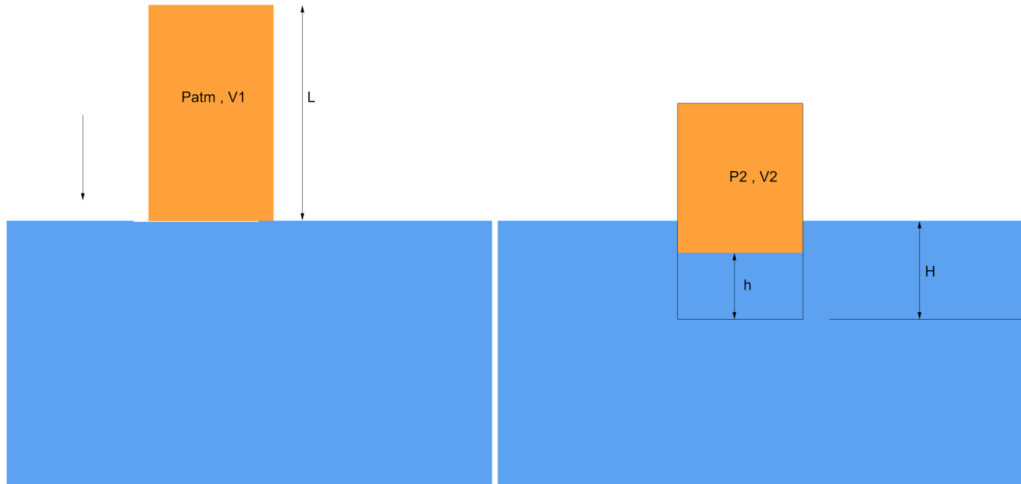


Figure 3.2: Lowering process schematic diagram

balanced by the hydrostatic pressure caused by the change in water level ( $H - h$ ). Ideal gas law gives a relation between the Pressure ( $P$ ), Volume ( $V$ ) and the Temperature of a gas. Here the air inside the suction anchor is considered as an ideal gas and it is assumed that the lowering process is adiabatic. As per ideal gas law, the relation between pressure and volume can be obtained as follows:

$$PV^\gamma = nRT \tag{3.1}$$

Where  $P$  is the air pressure,  $V$  is the volume under consideration,  $\gamma$  is the ratio of the specific heat,  $n$  is the mass of the air,  $R$  is the universal gas constant and  $T$  is the air volume temperature. The lowering process taken in this study is assumed as isothermal processes, so the value of  $\gamma$  is 1. The initial condition of the air phase and the suction anchor parameters are summarized in the Table 3.1

Suction anchor Mass	$M$	1.6kg
Suction anchor Length	$L$	0.3m
Suction anchor diameter	$D$	0.25m
Suction anchor cross section area	$A$	$0.049m^2$
Atmospheric Pressure	$P_e$	101325 Pa
Water Density	$\rho_w$	$1000 \text{ kg}/m^3$

Table 3.1: Model parameters

Boyle's law describes the relationship between pressure and volume of a gas, assuming the temperature remains constant. Since we are assuming an isothermal process, Boyle's law can be applied which yields:

$$P_1 V_1 = P_2 V_2 \quad (3.2)$$

Where  $P_1$  and the  $V_1$  is the initial pressure and volume and the  $P_2$ ,  $V_2$  is the final pressure and volume inside the suction anchor when it is under water. From the case above water,  $P_1$  is the atmospheric pressure ( $P_{atm}$ ) = 101325 Pa,  $V_1$  is the total volume of the suction anchor and for submerged state,  $P_2$  is the pressure inside the suction anchor, which is the sum of atmospheric pressure  $P_{atm}$  and the dynamic air pressure  $P_v$  where as  $V_2$  is the air volume after immersion. The air pressure inside the suction anchor in a immersed depth is equal to the hydro static pressure caused by the difference in water level inside and outside the suction anchor. Substituting these values in Boyle's law gives:

$$P_{atm} A L = (P_{atm} + P_{hydro}) A (L - h) \quad (3.3)$$

$$P_{hydro} = (H - h) \rho_w g$$

Substituting  $P_{hydro}$  in 3.3, we get:

$$P_{atm} A h = (H - h) \rho_w g A (L - h)$$

$$P_{atm} h = (H - h) \rho_w g (L - h)$$

Substituting the known values from Table[3.1] we get,

$$h^2 - h H - h L - \frac{P_{atm} h}{\rho g} + H L = 0 \quad (3.4)$$

Considering a case where the suction anchor is immersed into a depth of  $H = 0.25\text{m}$  and substituting the parameter values from Table [3.1] we get:

$$h^2 - 0.25 h - 0.3 h - \frac{101325 h}{1000 \cdot 9.8} + (0.25 \cdot 0.3) = 0 \quad (3.5)$$

which gives a value for  $h = 0.00689\text{m}$ . Which yields that when the anchor is immersed at  $H = 250\text{mm}$  into the water, the water level inside the suction anchor is 6.89 mm. The difference in water level will be 243.1mm which provides the hydrostatic pressure that is balanced by the weight of the suction anchor. Thus the pressure inside the suction anchor will be:

$$P_v = (H - h) \rho g = 2382.4 \text{ Pa}$$

This gives the net force acting on the suction anchor as ::

$$F_{net} = Mg - P_2 A$$

$$F_{net} = (1.6 \cdot 9.81) - (2382 \cdot 0.049) = -100.97 N$$

Thus in order to immerse the suction anchor up to a water depth of 0.25m, an extra mass of 10kg exceeding its self weight is to be added. Equation 3.3 can be used to simulate the water level inside the suction anchor , which can then be used to find the pressure and the net force acting on it.

### 3.1.4 Air Ventilation

When the suction anchor is lowered through water, the pressure inside it increases. If the vent valve is open, there is a pressure difference between the inside and outside of the suction anchor, which forces the air molecules near the high pressure side to enter the vent valve. As they pass through the vent valve and exit, they experience acceleration, leading to an increase in air velocity. This acceleration of air molecules through the vent valve results in decrease in pressure inside the suction anchor. This occurs because some of the pressure energy is converted into kinetic energy. This phenomenon is the air ventilation effect during suction anchor lowering which can be studied by calculating the pressure loss due to the increased air velocity.

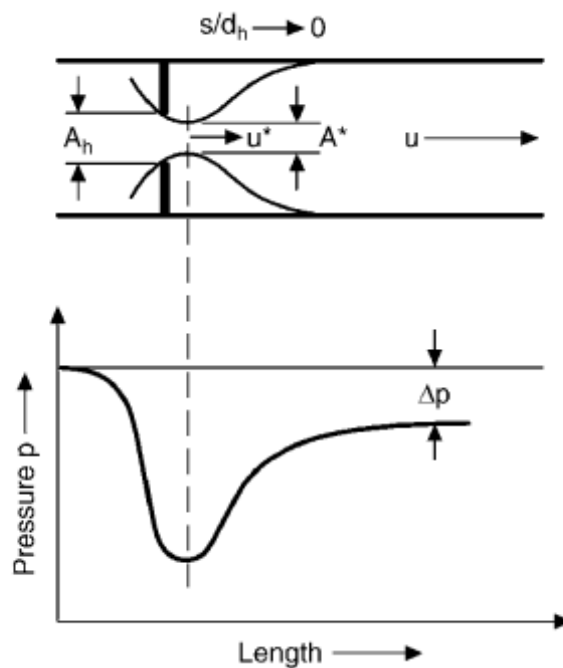


Figure 3.3: Pressure drop during fluid flow through orifice source - [7]

Figure 3.3 illustrates the fluid flow through orifice. According to the VDI Heat Atlas, Peter Stephan [7] in Section L1.7, when a fluid flows through vent in a pipe, it always undergoes a flow contraction that is followed by a flow expansion. During the flow contraction, the flow velocity increases and the static pressure decreases. No permanent pressure loss arises during flow contraction. During flow expansion after passing through the vent valve, the flow velocity decreases and

in turn static pressure increases(see Figure 3.3). Fluid flow in the direction of increasing pressure always results in a significant pressure loss. The permanent pressure loss  $\Delta P$  can be calculated using Borda-Carnot equation given in VDI Atals [7] which is given by:

$$\Delta p = \frac{\rho}{2} \cdot (V_2 - V_1)^2 \quad (3.6)$$

Where  $\rho_a$  is the density of air ( $1.293 \text{ kg/m}^3$ ),  $V_1$  is the suction anchor velocity and  $V_2$  is the air flow velocity through the vent. Thus the permanent pressure loss is proportional to the square of the velocity difference before and after flow expansion. The velocity after flow expansion  $V_2$  can be found out by calculating the volumetric flow through an orifice which is given by Equation 2.6 in section 2.2.4. Equation 2.6 is derived by applying Bernoulli's equation and continuity equation for a flow through orifice. Volumetric flow  $Q_v$  of air flowing through the vent valve is, the area of the vent  $A_2$  multiplied by the velocity of the air through the vent  $V_2$ . By substituting these values in to Equation 2.6, the flow velocity through vent can be calculated as:

$$A_2 V_2 = C A_2 \sqrt{\frac{2(P_1 - P_2)}{\rho}}$$

$$V_2 = C \sqrt{\frac{2(P_1 - P_2)}{\rho}} \quad (3.7)$$

In Equation 3.7,  $(P_1 - P_2)$  is the pressure difference between inside and outside of the suction anchor which is  $(H - h)\rho_w g$  as per Equation 3.3. Substituting the pressure difference into the velocity equation yields:

$$V_2 = C \sqrt{\frac{2(H - h)\rho_w g}{\rho}} \quad (3.8)$$

Substituting Equation 3.7 in to Equation 3.6, the modified pressure loss equation is formulated as:

$$\Delta p = \frac{\rho}{2} \left( C \sqrt{\frac{2(H - h)\rho_w g}{\rho}} - V_1 \right)^2 \quad (3.9)$$

where C is the orifice flow coefficient which is given by

$$C = \frac{C_d}{\sqrt{1 - \beta^4}}$$

$C_d$  is the discharge coefficient of the orifice plate which is taken to be 0.61 (as per chapter L1.7 section 1.4 in VDI Atlas [7] ) and  $\beta$  is the ratio of orifice hole diameter to pipe diameter which is calculated to be 0.016.

Equation 3.9 describes the pressure loss due to the air ventilation during suction anchor lowering. This equation is used to find the net pressure inside the suction anchor during lowering with the valve open.

### 3.1.5 Wire stiffness force

As mentioned in 3.1.1, the weight of the suction anchor causes the lifting wire to get elongated to some extent. This generates a restoring upward force in the lifting wire which can be calculated as:

$$F_{spring} = k \Delta L \quad (3.10)$$

where the stiffness of wire  $k = \frac{AE}{L_0}$  and  $\Delta L$  is the elongation of the lifting wire. The stiffness of the lifting wire is the ratio of axial stiffness  $EA$  to the unstretched wire length  $L_0$ .

### 3.1.6 Added mass and Damping force

When the suction anchor is lowered into the water, there will be an apparent increase in mass experienced by the suction anchor due to the surrounding fluid's inertia which always opposes the motion of the anchor. The added mass force when lowering in still water is proportional to the acceleration of the body. Apart from the added mass force, there will be drag force exerted by the fluid on the anchor. The Equation for the added mass and drag force is given by the Morison Equation. Which is used to calculate the wave forces on slender cylinder as per of Sea Loads on Ships and Offshore Structures by Faltisen [2] (see page 61).

$$F = C_m \frac{\pi d^2}{4} \rho \ddot{x} + \frac{1}{2} \rho C_d D |\dot{x}| \dot{x}$$

Here the first term is the added mass term which is proportional to the acceleration of the body. The inertia coefficient  $C_m = 1 + C_a$  contains both Froude Krylov forces and Diffraction forces. Since the study considers still water the Froude Krylov force can be neglected. So the Added mass and Drag forces will be as shown below:

$$F_{AM} = C_a \frac{\pi d^2}{4} \rho \ddot{x} \quad (3.11)$$

$$F_D = \frac{1}{2} \rho C_d D |\dot{x}| \dot{x} \quad (3.12)$$

Where  $C_d$  is drag coefficient of the suction anchor. The added mass and drag coefficient of the suction anchor for lowering can be found out from DNV RPH103 [1]. The Drag force for the suction anchor for vertical motion will be negligible as the reference area cross section perpendicular to the flow is very small. A simplified approximation of the added mass coefficient is mentioned in section 2.2 of the paper presented by Lixin Zhu and Hee-Chang Lim [8]. In the paper heave added mass of a submerged vertical circular cylinder is approximated as the mass of a hemisphere as shown in figure 3.4.

$$A_{33} = \frac{2}{3} \pi r^3 \rho_w$$

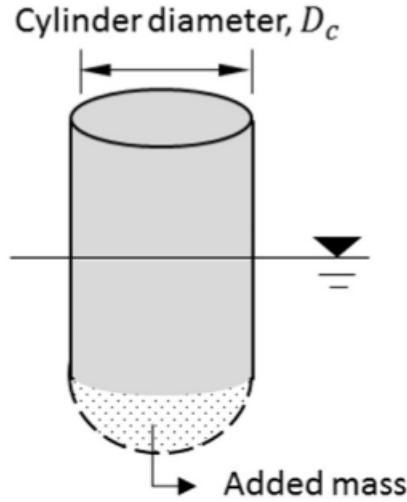


Figure 3.4: Approximate added mass of a semi submerged vertical cylinder source- [7]

Thus the added mass force when the suction anchor is lowered into the water is given by:

$$F_{AM} = \frac{2}{3} \pi r^3 \rho_w \ddot{x}$$

However, it is important to note that the drag force is less prominent for the lowering process as it is just a ring that can contribute to form drag and the skin friction drag is acting only in a small surface area

### 3.1.7 Slamming Force

Slamming force refers to the impact force experienced by the body when it hits the water surface. The slamming force can also be defined as rate of change of added mass fluid momentum. During a slamming event, the sudden change in fluid pressure results in a rapid deceleration of the body. This change in motion triggers significant added mass forces, which can amplify the slamming force experienced by the body. The calculation of slamming force during lowering of an object can be complex and depends on various factors, including velocity of the object, the shape and the size of the object, water depth and the characteristics of the fluid. DNV-RP-H103 [1] specifies a formula for calculating the slamming force of an object lowered through the free surface with slamming velocity  $v_s$  in still water.

$$F_s(t) = \frac{1}{2} \rho_w C_s A_p v_s^2 \tag{3.13}$$

where  $C_s$  is the slamming coefficient calculated as:

$$C_s = \frac{2}{\rho_w A_p v_s} \frac{dA_{33}^\infty}{dt} \tag{3.14}$$

Where  $\rho_w$  is density of water [ $kg/m^3$ ]

$A_p$  is the horizontal projected area of object [ $m^2$ ]

$h$  is the submergence relative to surface elevation [m]

$\frac{dA_{33}^\infty}{dt}$  is the rate of change of heave added mass with submergence.

For a suction anchor lowering process the slamming can occur two times. The first entry of the suction anchor to the water can be related to slamming effect. But this is not that severe because the surface entering water is just a ring. It might have some considerable slamming effect if it was closed at the top. But there is air inside it which is a bit compressible and also the air gets ventilated through the vent valve leading to a reduced slamming force. The second slamming occurs when the top plate of the suction anchor impacts the water surface. This "secondary" slamming related to a classical problem in hydraulic pipe flows where the slamming occurs when the fluid hits the dead end of the pipe creating a hydraulic hammer shock. It can be reduced by some design changes in the suction anchor such as a conical top or top plate with a shape of a hemisphere to reduce the effective area. This effect is not considered in this study, rather the focus was on the 1st entry into the water. Additionally, the assessment of this secondary slamming force can not be achieved in the present experimental setup as it will be a huge force of magnitude out of the range of force sensor used and also the force sensor cannot measure the upward force. This force will be difficult to be included in the simulation model. Thus the experiments will be conducted for lowering until just before the suction anchor top hits the water.

### 3.1.8 Simulation model

All the forces and their corresponding equations discussed in the previous sections are combined to formulate the suction anchor equation of motion (ODE) which is given by:

$$(M + A) \ddot{x} = Mg - ((H - h)\rho_w g - \Delta p)A - \nabla \rho_w g - \frac{1}{2} \rho_w C_d A v \cdot |v| - \frac{1}{2} \rho_w C_s A_p v^2 - k \cdot \Delta l \quad (3.15)$$

Mass + Added Mass points to  $(M + A)$   
Buoyancy points to  $\nabla \rho_w g$   
Drag force points to  $\frac{1}{2} \rho_w C_d A v \cdot |v|$   
Slamming Force points to  $\frac{1}{2} \rho_w C_s A_p v^2$   
Spring force points to  $k \cdot \Delta l$   
Force from net air pressure points to  $((H - h)\rho_w g - \Delta p)A$

Where,

$$A = \frac{2}{3} \pi r^3 \rho_w$$

$$\Delta p = \frac{\rho_a}{2} \left( C \sqrt{\frac{2(H - h)\rho_w g}{\rho_a}} - v \right)^2$$

M - mass of the suction anchor

$\Delta p$  - pressure loss due to air ventilation as per Eq 3.9

A - Approximated heave added mass of the suction anchor

$\rho_w$  - Density of water

$\rho_a$  - Density of air in

$\ddot{x}$  - Heave acceleration of the suction anchor

r - Radius of the suction anchor

v - Velocity of the suction anchor  $\rho$  - Density of water in  $kg/m^3$

$\nabla$  - under water volume of the suction anchor that offer water buoyancy

$C_d$  - Drag coefficient of the suction anchor cross section

g - acceleration due to gravity

H - Water height outside the suction anchor

h - Water height inside the suction anchor

$\mu$  - Stiffness of the lifting wire

$\Delta l$  - elongation of the lifting wire.  
 k- Stiffness of the lifting wire  
 C - Orifice flow coefficient

Proper simplification were applied on the formulated suction anchor equation of motion (Equation 3.15), to create a python code for simulating the obtained ordinary differential equation. The motion equation was solved using python ODE solver "solve\_ivp" in Scipy Python library that uses 4<sup>th</sup> order Runge–Kutta method. The position, velocity, air pressure and force plots are extracted from simulation results for comparison with the experimental data. Appendix A shows the python code for simulation of the suction anchor lowering process . Figure 3.5 shows the simulation results for lowering of suction anchor with the valve closed.

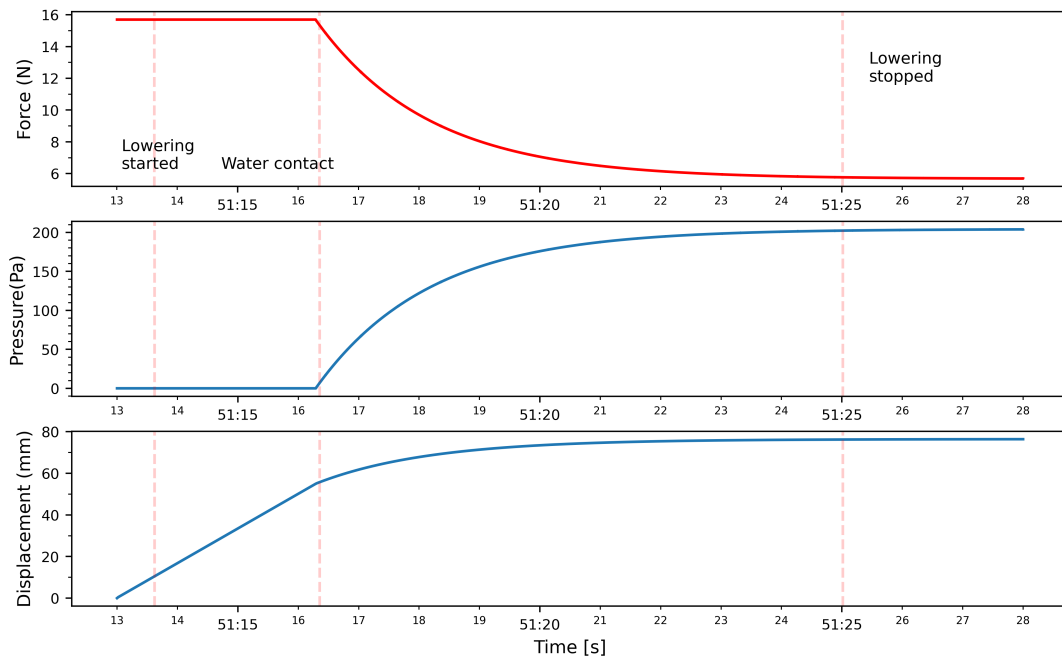


Figure 3.5: Wet closed Simulation results



## 3.2 Experimental Method

A scaled down model of the suction anchor is made to carry out the experiments in the towing tank at NTNU Ålesund. The model dimensions are made with a D/H ratio of 0.8 that matches with real world suction anchors used in the industry. A crane on the side of the towing tank enables the suction anchor to be lowered, while sensors record the net-force, position and pressure within it. These sensors are carefully calibrated to ensure accurate measurements. Furthermore an integrated data acquisition system is designed for synchronous sensor measurements. Once the the experimental setup is made working, an experiment plan with a test matrix is prepared to evaluate each forces discussed in section 3.1.1. These measurement data for each test case will be used to validate the developed analytical model.

### 3.2.1 Existing setup / Facilities

The study utilized the towing tank facility available at NTNU Ålesund for conducting the experiment. The tank has a length of 10.9m, the width is 2m and a depth of 0.8m. The wave tank has a crane that is mounted on its side and a DC motor was installed to behave as a working crane model. The DC motor is connected to a voltage source regulator for adjusting the hoisting speed.

### 3.2.2 Experimental test setup development

The initial concept of the experimental setup is shown in the Figure 3.6. The crane boom and DC motor is used to duplicate a working crane model. A wheel drum is fitted to the rotor which acts like a winch to lower and raise the suction anchor model. A magnetic encoder that measures the angular increment, is fitted to the wheel drum. This is to measure the position of the suction anchor. The net force acting on the lifting wire is measured using a force sensor that is placed under the lifting boom of the crane. To investigate the entrapped air effect, the pressure developed inside the anchor needs to be measured. This is achieved by the use of a digital pressure sensor which is placed inside the suction anchor. A measurement circuit setup is designed to integrate all the sensors together for synchronous measurement and logging of the sensor data. Within the circuit, the sensors are connected to micro-controllers, ESPWROOM-32 and RaspberryPi, for integrated sensor data logging. The final experimental setup is presented in Figure 3.7.

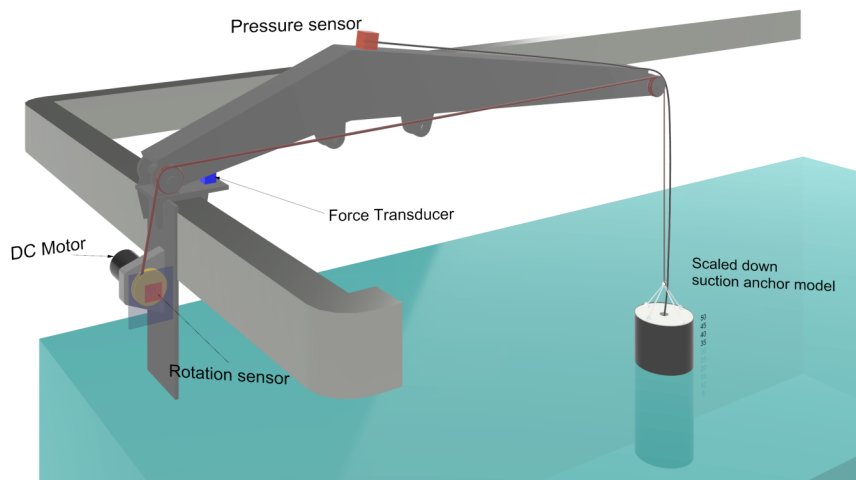


Figure 3.6: Experimental Setup - Initial Concept

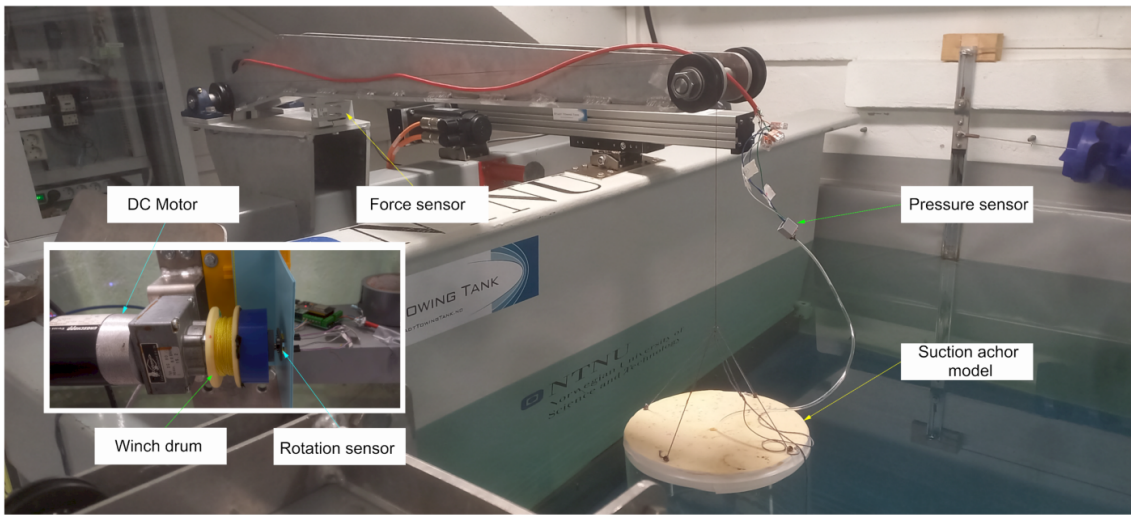


Figure 3.7: Final Experimental Setup

### Sensor Measurement Setup

Below listed are different sensor devices that are used for acquiring measurements for the experiments.

- Force sensor - HBM S2M 1000N + HX711 + Analog to digital Converter (ADC)
- Rotation sensor - AS5600 - Magnetic encoder
- Pressure sensor - HX710b

These sensors measure the physical quantity and generate analog electrical signals. The analog signals are then amplified and filtered using an electronic scale module. HX711 module is used as the scale module for the force sensor. The pressure sensor HX710b already comes with HX711 module which could be directly connected to the micro-controller. The principle concept for single sensor measurement setup is shown in Figure 3.8.

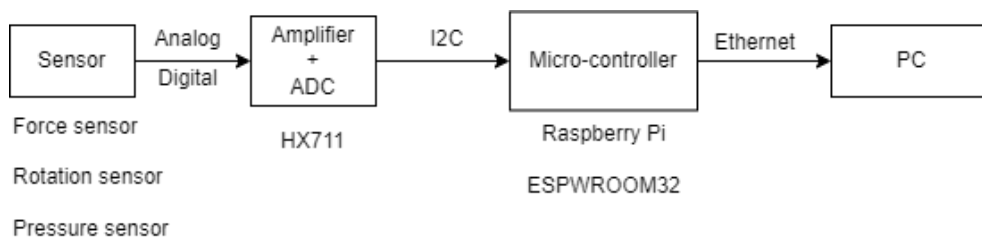


Figure 3.8: Sensor measurement setup - Principle concept

Since the measurements from all the sensors are to be synchronized, a multi sensor measurement configuration is adopted to eliminate interruptions during measurement logging. A simplified diagram is shown in Figure 3.9 .

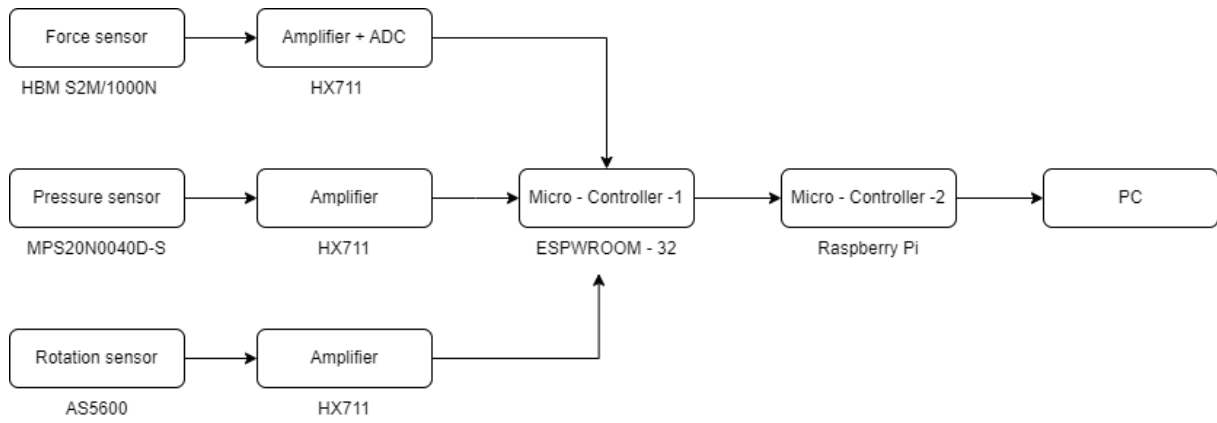


Figure 3.9: Multi-sensor measurement circuit setup

### 3.2.3 Sensor devices

Once a working sensor measurement setup with synchronized logging is achieved, all sensors should be calibrated with a known measurement of the physical quantity to have accurate measurement results. The following subsection discusses on various sensor devices that are used for the experiments.

#### Pressure sensor

The pressure sensor used for this study is HX710b pressure sensor module. It is an integrated module consisting of MPS20N0040D-S pressure sensor and HX710B analog to digital converter. It can measure a pressure range from 0-40kPa. Figure 3.10 shows the picture of the pressure sensor. The sensor is calibrated by taking hydrostatic pressure as the reference pressure. The measured value had a gain correction factor of 0.925 Pa/m of water depth and an offset of -65.26 Pa. The sensor calibration plot is shown in figure 3.11.

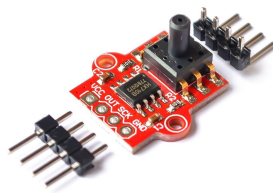


Figure 3.10: HX710B pressure sensor module  
source- [www.electroschematics.com](http://www.electroschematics.com) [3]

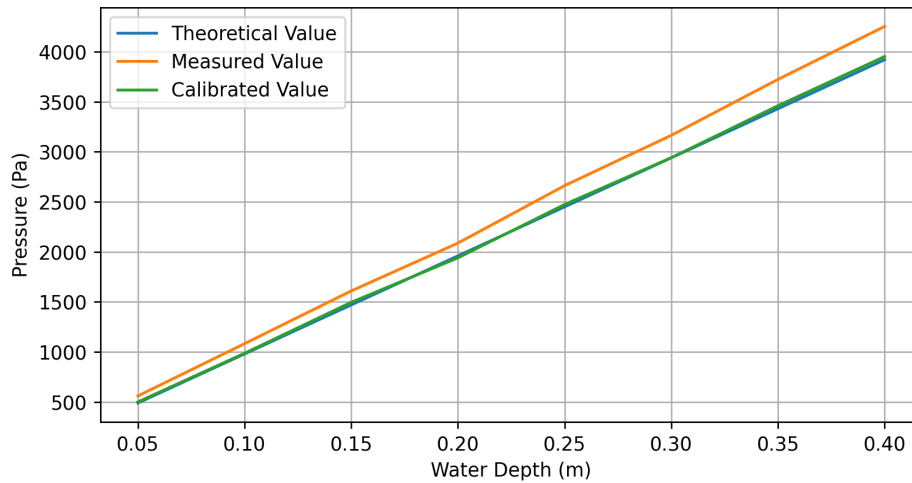


Figure 3.11: Pressure sensor calibration

After correcting the measured value with gain correction factor and offset, the calibrated values were found to match the theoretical hydrostatic pressure values for different water depths with a tolerance of 0.6%.

### Force sensor

An HBM S2M/1000N force sensor is used for the experiments which produces analog measurement signals. It is then converted into a digital signal using HX711 module which is an analog-to-digital converter. The force sensor is calibrated with known reference weight. Figure 3.12 shows the picture of the force sensor.



Figure 3.12: Force sensor  
source- [www.hbm.com](http://www.hbm.com) [5]

### Rotation sensor

The rotation sensor used in this experimental setup is AS5600, which is a magnetic encoder that measures the angular increments with the use of dipolar magnet.

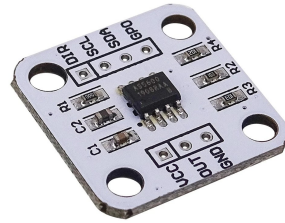


Figure 3.13: Rotation sensor AS5600  
source - [www.ams.com](http://www.ams.com) [4]

The linear position of the suction anchor is calculated from the angular increments measured by the magnetic encoder fitted on the wheel drum. Figure 3.14 shows the rotation sensor arrangement for measuring position of the suction anchor. The calculated linear displacements are then calibrated with known displacements.

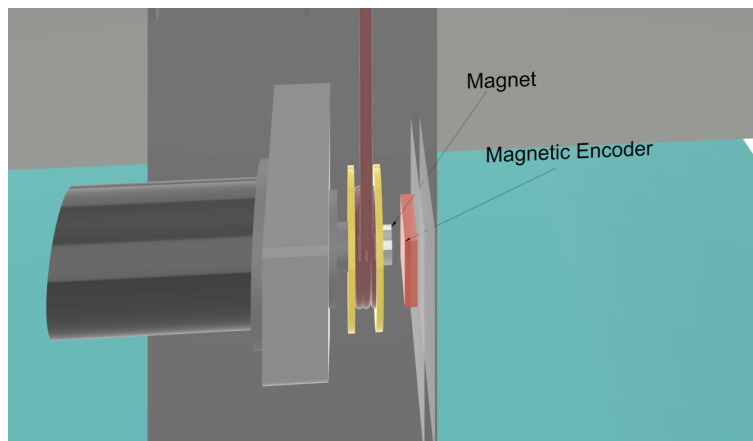


Figure 3.14: Rotation sensor setup

### 3.2.4 Design and build test specimen

The diameter to height ratio of the test model was decided with reference to the practical dimension range used in the industry. Initially a test model of D/H ratio of 0.8 and a hole diameter to outer diameter ratio of 0.2 was selected to carry out the experiment. A typical test specimen representation is shown in Figure 3.15

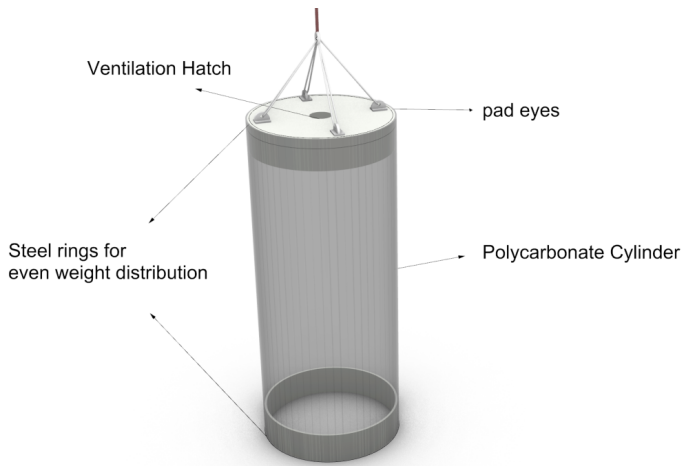


Figure 3.15: Test specimen

Weight	1.67kg
Height	0.3m
Diameter	0.25m
D/H	0.83
Area	0.049 m <sup>2</sup>
Thickness	4mm

Table 3.2: Principle dimension

### 3.2.5 Experiment Plan

Once the experimental setup is made working, an experimental plan is made to study the forces acting on the anchor while lowering. To formulate the mathematical model, it is important to decompose the whole lowering process into simplified experiments to examine the contributions of each forces. By decomposing and isolating each forces, a better knowledge of the anchor behaviour could be achieved and also helps to determine the factors that affects its motion. The important parameters of the dynamic air pressure and hydrodynamic forces acting on the suction anchor have to be investigated. The experiments are broadly divided into static and dynamic experiments.

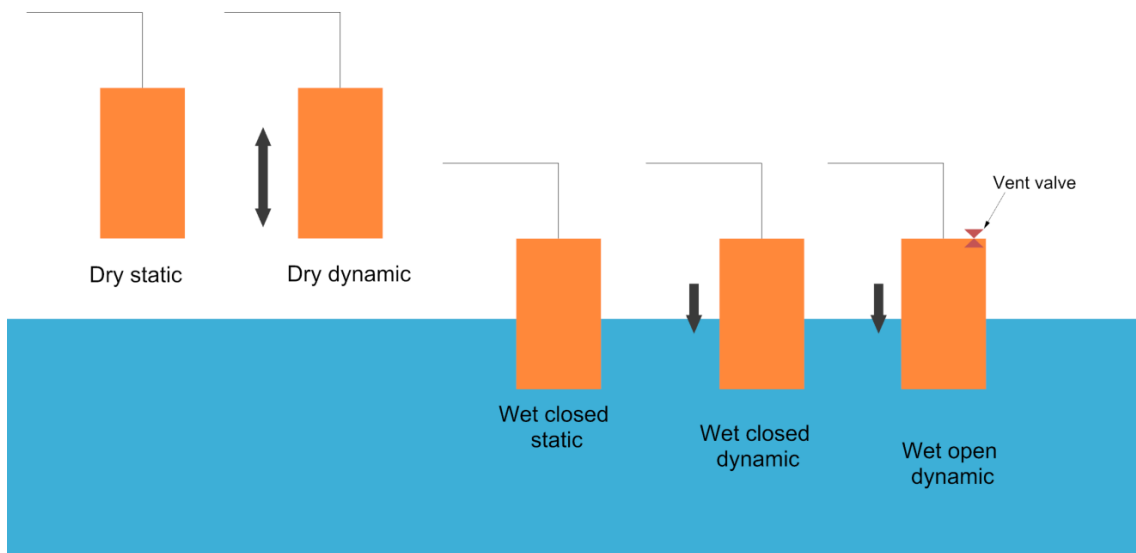


Figure 3.16: Experiment Plan

**Dry static**

This test is carried out to calibrate the force sensor. The suction anchor model is suspended in air using the crane, to measure its self weight on the force sensor. A series of force measurement is made for different known weights, to calibrate the force sensor and calculating the gain and offset values. Figure 3.17 shows the calibration plot for the force sensor. The obtained measurement value had a gain correction factor of 0.919 N/kg and an offset 0.441N. After the calibration the dry weight of the suction anchor was measured to be 16.7N.

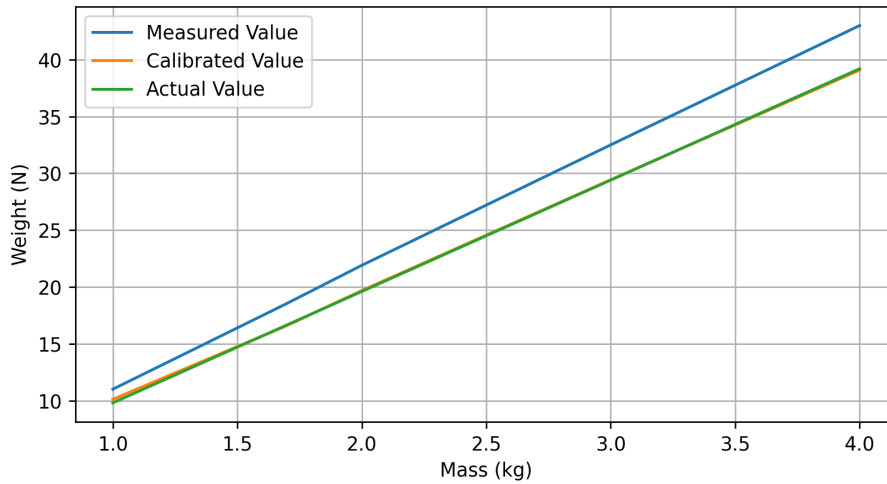


Figure 3.17: Force sensor sensor calibration

**Dynamic Dry**

This experiment is performed to study the stiffness of experimental setup. The suction anchor is lowered in air with a velocity and then made to stop. The force and position data of the suction anchor is recorded. To further investigate the characteristics of the experimental setup, a Fourier analysis is conducted in the frequency domain. The analysis is performed to find out the heave natural frequency of the suction anchor lifting setup. The purpose of conducting the Fourier analysis is to identify and eliminate any unwanted heave oscillations during lowering measurement. Since only heave motion is considered in this study, the analysis helps in filtering out or minimizing any undesired heave oscillations that may occur due to resonance during the lowering process.

Figure 3.18 shows the position plot of the dry dynamic test and Figure 3.20 displays the Fourier analysis performed on the time series position data to find out the natural frequencies. It was observed in Figure 3.20 that there is a peak at zero frequency which signifies the non oscillating component and represents the static state of the system, which can be ignored. Furthermore an increase in amplitude is observed at  $\omega = 0.75$  Hz which can be considered as the natural frequency. It's important to note that this approach assumes that the dominant frequency obtained from the Fourier analysis corresponds to the natural frequency of the heave motion of suction anchor. In some cases, there may be multiple frequency components present in the data due to different system modes or external factors. In such cases, a more advanced spectral analysis or modal analysis techniques may be required to accurately identify the natural frequency.

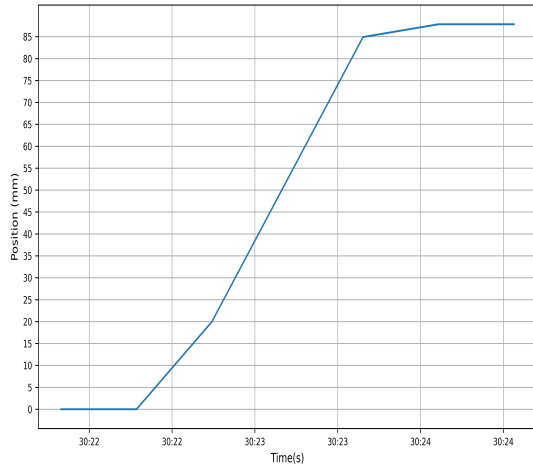


Figure 3.18: Dynamic dry - Position plot

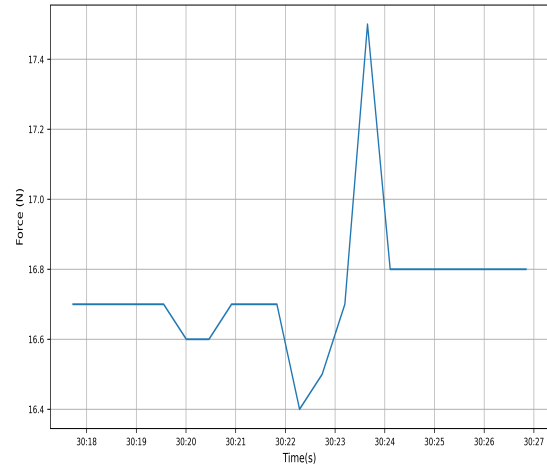


Figure 3.19: Dynamic dry - Force plot

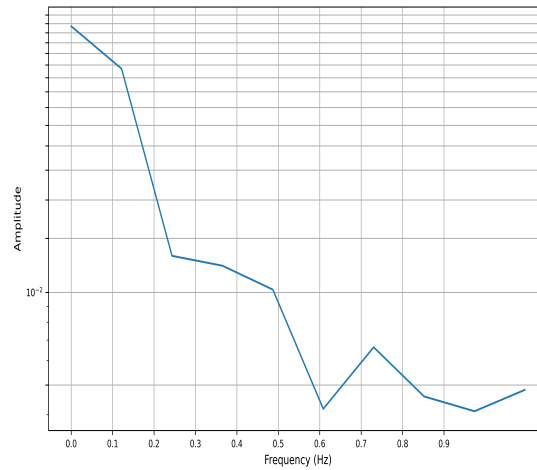


Figure 3.20: Fourier analysis - position data

From the obtained natural frequency, the stiffness of the lifting system can be calculated as:

$$\omega = \frac{1}{2\pi} \sqrt{\frac{K}{M + A}} \tag{3.16}$$

where  $\omega$  is the natural frequency in Hz, K is the stiffness in heave (N/mm) and M is the mass in kg and A is the added mass of the suction anchor. The stiffness of the lifting system at the natural frequency for mass M is calculated as:

$$K = 4\pi^2 \omega^2 M = 35 \text{ N/m} = 0.035 \text{ N/mm}$$

The stiffness of the heave motion is provided by the lifting wire. The axial stiffness of the lifting line is given by:

$$K_l = \frac{AE}{L}$$



The rope used for the experiment was a nylon rope with  $E = 2.7\text{GPa}$  has a diameter of 2mm and length of 0.6m which gives a stiffness value of 14.13N/mm which is far beyond the stiffness value found from the measurement data. Thus the unwanted oscillation due to natural frequency in the measurement data is ruled out.

**Wet closed static**

This experiment is conducted to determine the static depth for different suction anchor weights when lowered with valve vent closed. Figure 3.21 illustrates the experimental measurement plot and its comparison with theoretical values calculated from the static forces. Multiple attempts have been made to obtain more accurate measurements and a linear trendline has been added to compare the experimental measurements. The experimental data will then later be used to compare with the simulation results of the mathematical model. It is observed from the Figure3.21 that the trendline of the experiment data is close to the theoretical value. The maximum variation was found to be 2cm which could be due to the air compressibility or the unaccounted water buoyancy force from the underwater enclosed volume of suction anchor.

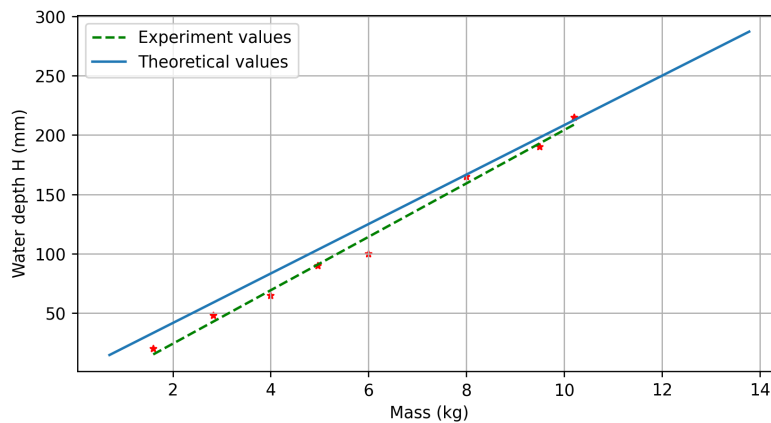


Figure 3.21: Wet closed static - Depth measurement

Additionally, same tests were carried out to measure the pressure developed within a suction anchor when lowered into water. The pressure data is then compared with the theoretical values calculated from the static forces. The inside pressure is measured for a range of suction anchor weights and the comparison plot is shown in Figure 3.22. It is observed from the plot that, there is a constant pressure offset of 170Pa for every pressure readings which could be due to some inaccuracies in pressure sensor measurements or due to uneven weight distribution on the suction anchor model, that makes it to get tilted before the maximum pressure is attained. This offset is taken into account when the experimental results are compared with the simulation results later.

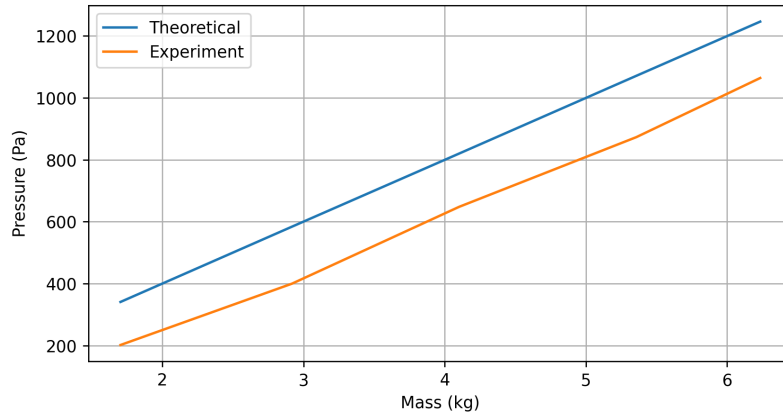


Figure 3.22: Wet closed static - Pressure measurement

**Wet closed dynamic**

This experiment is performed to evaluate the dynamic pressure developed inside the suction anchor during lowering. It also includes the hydrodynamic forces such as added mass, drag and slamming forces acting on the suction anchor. This test case is carried out with valve closed to exclude the air ventilation effect when lowering.

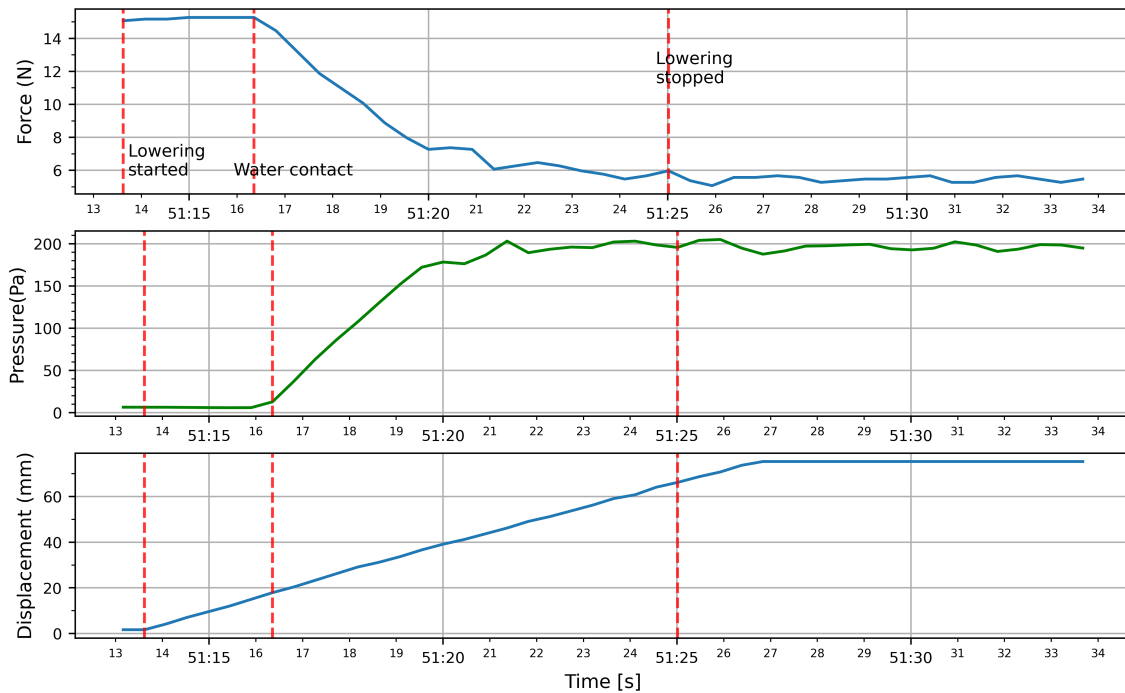


Figure 3.23: Wet closed dynamic

Figure 3.23 indicates the experimental results for the dynamic wet closed test case. It is evi-

dent from the graph that, once the suction anchor touches the water line, the inside air pressure of the suction increases to give an upward buoyancy which leads to a reduction in force measurement on the lifting line. Apart from the buoyancy due to trapped air, the hydrodynamic forces also contribute to the force measurement.

**Wet open dynamic**

This experimental test case is performed to evaluate the pressure drop due to air ventilation effect during suction anchor lowering. The experiment is performed by lowering the suction anchor model into water, keeping the vent valve open. The position, force and pressure on the suction anchor during lowering is measured until the still water level is beneath the suction anchor top plate. This is to evaluate the air ventilation effect by eliminating the measurement peaks due to slamming force from water impact on the top plate. Figure 3.24 shows the measurement plots of position, net-force and air pressure recorded during the lowering process. Here the suction anchor model is lowered at a speed of 13mm/s. From the measurement plot, it is observed that there is a gradual increase in pressure, once the suction anchor comes in contact with the water surface. The developed pressure includes both the static pressure from the closed valve case as well as the pressure drop due to ventilation. The pressure then approaches to atmospheric pressure after the lowering is stopped. The measurements are later compared with the simulation results of the mathematical model.

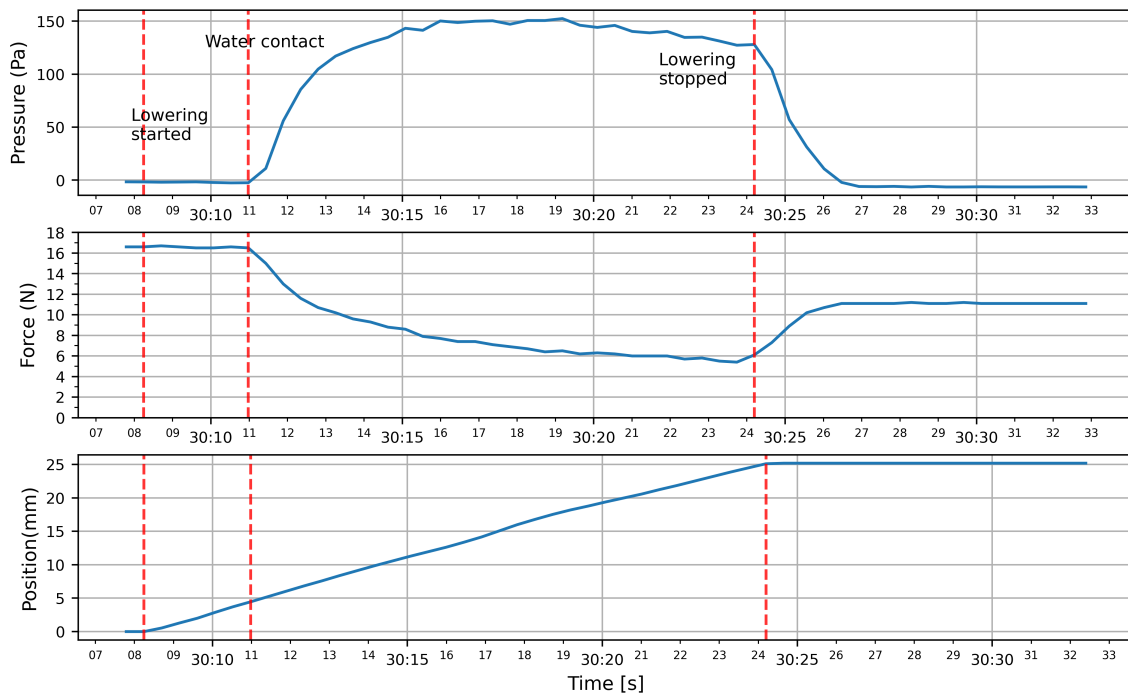


Figure 3.24: Wet open dynamic

# Chapter 4

## Results and Comparison

### 4.1 Validation of simulation model

#### Wet closed static

In order to validate the analytical model developed in section 3.1.8, the first step is to compare its static results with the experimental data. Multiple simulations were carried out with different suction anchor weights to extract the final water depths at which it floats. The obtained values from simulated results are compared with the experimental measurements for wet closed static case shown in section 3.2.5. Figure 4.1 shows the comparison plot for water depth from simulation results and the experimental measurements for wet closed static case. From the plot it is observed that the simulated water depth has a good agreement with the experimental measurements. The maximum variation was found to be less than 2cm. However the small variation could be due to the reading error while taking the experimental data.

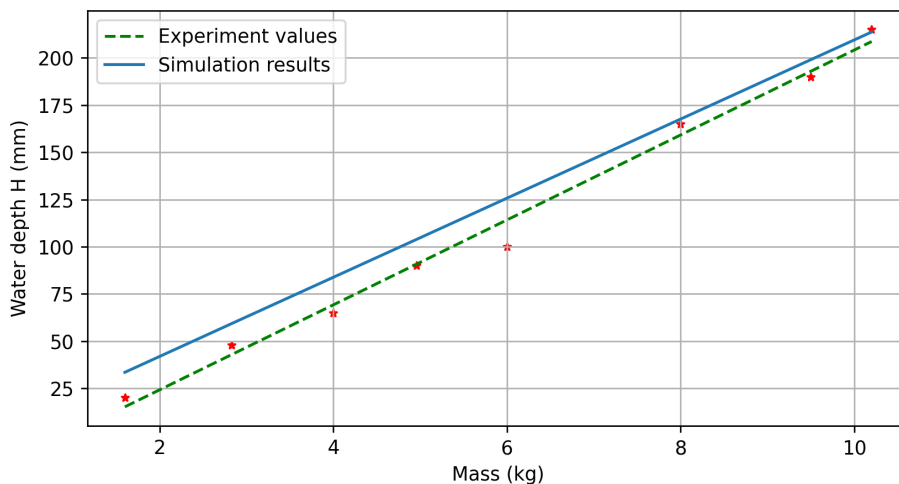


Figure 4.1: Simulation model validation - Static water depth

Additionally, the simulated pressure developed inside the suction anchor is compared with the pressure sensor data obtained from the experiment. Multiple simulations were carried out to extract the final pressure value for a range of suction anchor weights. Figure 4.2 shows the pressure comparison plot for different suction anchor weights. It is noticed that there is a good agreement between the simulated and experimental pressure value. The maximum variation of the simulated pressure with the pressure sensor data was found to be 50Pa. From the comparison plot it can be concluded that the simulation model well describes the wet static model of a suction anchor in water.

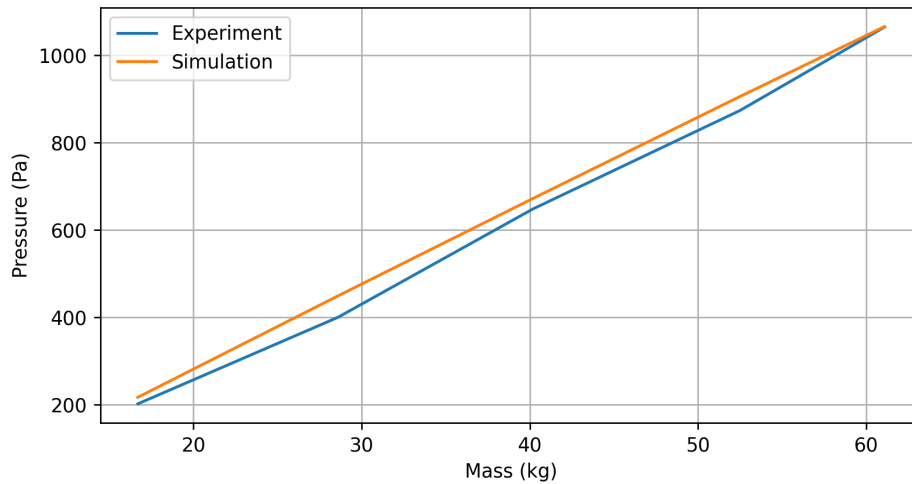


Figure 4.2: Simulation model validation - Static pressure

### Dynamic wet closed

Once the static results of the simulation are validated with the experimental measurements, the next step is to compare the dynamic behaviour of the suction anchor. For the dynamic wet closed test case, in addition to the forces that are acting in the static test case, there will hydrodynamic forces such as added mass, drag force as well as the slamming force which occurs during the first contact with the water. So this validation is performed to see if the hydrodynamic forces are modelled correctly in the simulation model. Experimental results from the section 3.2.5 is compared with the simulation model results. To compare both the results, it is important that the simulation as well as the experiment should start lowering at the same time and lowered with the same speed. Also, the self weight and vent valve size of both the models should be identical. Figure 4.3 shows the comparison plot. It is noticed from the plot that, there is a reasonable agreement between experimental and simulated results for pressure and force acting on the suction anchor. It is observed that there is some slight variations for the position and velocity data measured using both the methods. A potential explanation for this variation could be an error in the measured position data during the experiment. The experiment data was measured from the beginning of the lowering process until the suction anchor experiences a tilt, at which point the net force was approaching zero due to the upward force from trapped air. It is conceivable that the lowering might have continued for an additional 30mm after the tilt occurred, which could be a reason for the offset in the static depth.

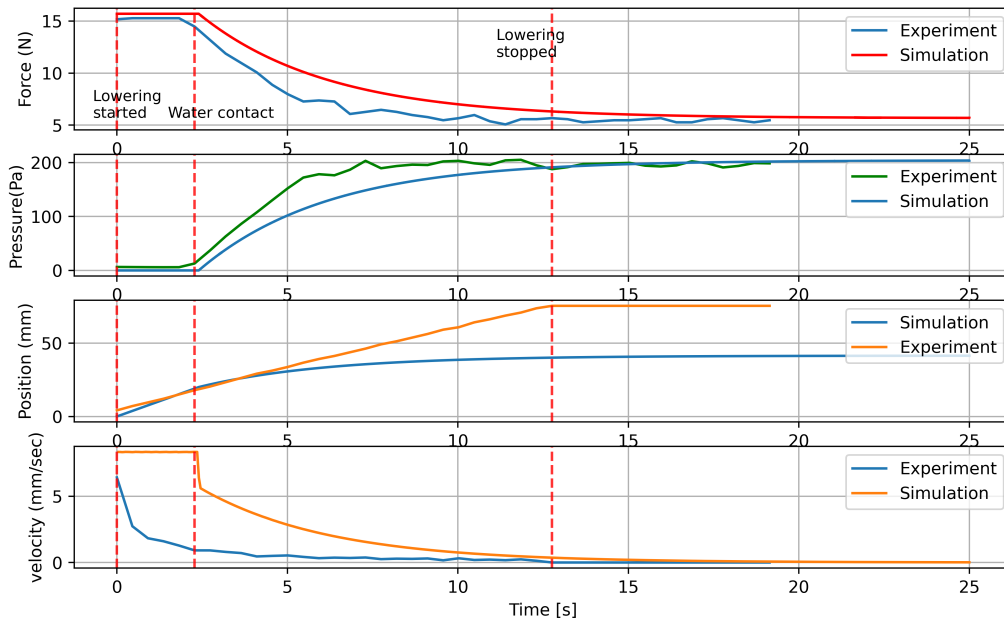


Figure 4.3: Wet closed dynamic

### Dynamic wet open

The simulation results for the dynamic wet open case is compared to the experimental measurements. Figure[4.4] shows the comparison plot. Looking at the experimental measurements, it was noticed that the pressure increased to around 190Pa as the suction anchor make contact with the water. This pressure increase can be due to the build up of static pressure within the anchor. As a consequence a decrease of 10N in the net force was observed. Subsequently, a gradual decrease in pressure was observed, potentially caused by the pressure drop due to air ventilation through the vent valve. Additionally, it was also noted that pressure curve continues to decrease even after the lowering process has stopped which can be accounted to the continued air ventilation which attempts to equalize the pressure both inside and outside the suction anchor. From the comparison plot, it was observed that there is a clear mismatch in the velocity and position curves between experiment and simulation. The simulation model was tuned to have a fair match in the final position. But there was considerable variation in the velocity data. However looking at the pressure and force comparison curves, it was observed that the final values in the simulation model results had a good match with the extreme values in the experimental pressure and force data. The variation in the transient phase might be due to the approximations or simplification adapted in the simulation model or there might be some effects that were not considered while formulating the mathematical model. This mismatch was noticed in the late stages of the thesis work and a proper validation has not been able to achieve.

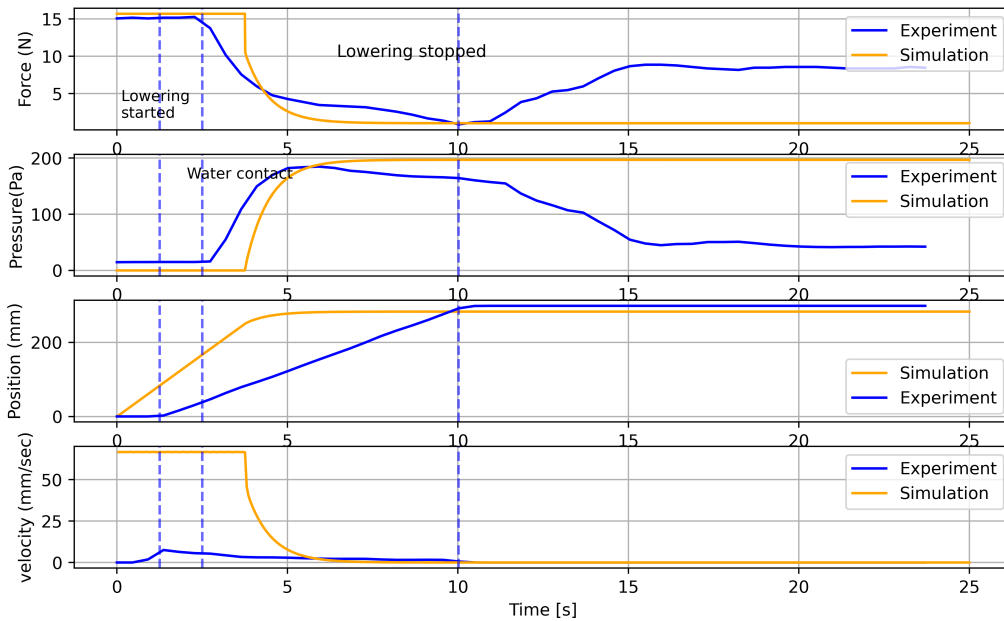


Figure 4.4: Wet open dynamic

## 4.2 Parametric study

The developed experimental setup was used to conduct the parametric study of the vent valve size and lowering velocity to see how it influences the behaviour of the suction anchor while lowering into water. The findings of the study can be used to predict the influence of lowering velocity and vent valve size on the behaviour of suction anchor when it is lowered into water and will be useful to discuss potential improvements to the lowering process.

### 4.2.1 Changing lowering velocity

Experiments were conducted on the selected suction anchor model with different lowering velocities for a constant vent valve size. The changes in the force and pressure measurement were measured and compared. Figure 4.5 shows the comparison plot. It is observed that the upward force due to air pressure increases with lowering speed. From the curves for lowering speed 3.34 mm/sec and 2.262 mm/sec, the upward force seems to come quite close to the suction anchor weight and the net force is observed to be approaching zero. From this it can be inferred that insufficient air ventilation and increased lowering velocity can result in zero or almost zero net force, which can cause the lifting line of slings to become slack. Thus the entrapped air effect can be significant to take into account for suction anchor lowering analysis. However, for suction anchor lowering with 0.6 mm/sec speed, it is observed that there is no considerable upward force developed which can create a potential slack in the lifting wire. But this velocity is too small for the lowering operation.

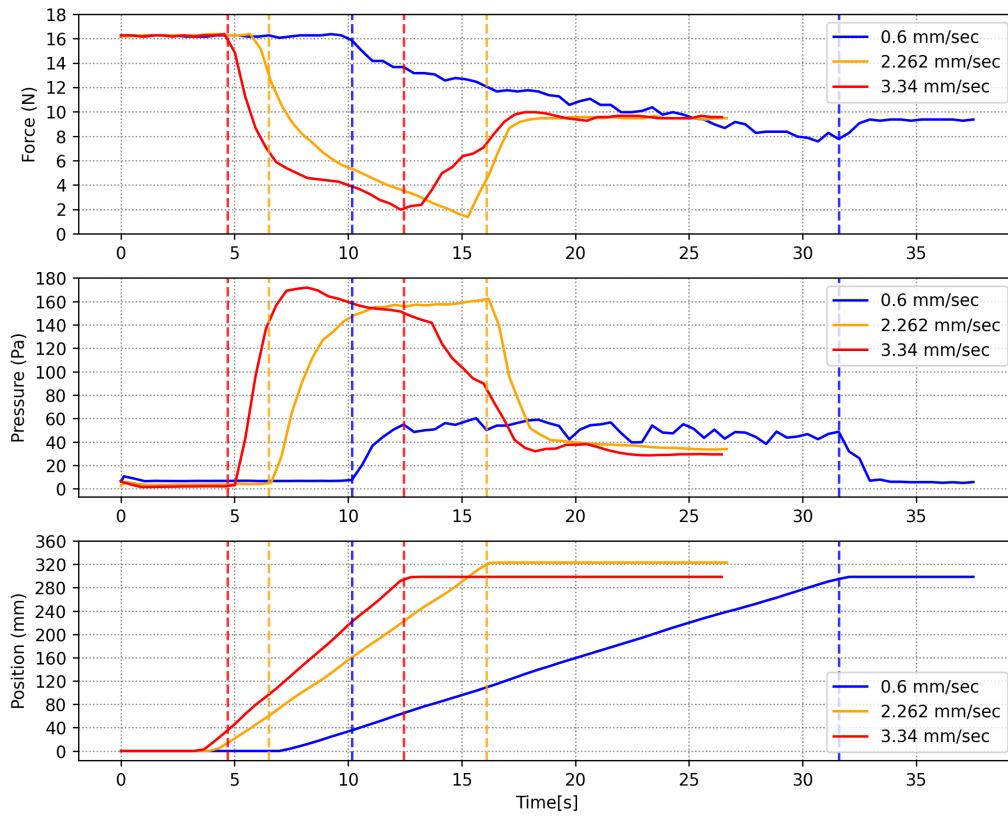


Figure 4.5: Varying lowering velocity for constant hole size

### 4.2.2 Changing Vent valve size

To study how the vent valve size affects the pressure and force measurements, lowering experiments with different vent valve sizes are performed. For comparing the effect of vent valve size, the lowering should be performed at same velocity for all the tests. Figure 4.6 shows the comparison plot for lowering velocity. The velocity was observed to be matching for both the simulation and experiments. Once the velocity is matched, the comparison for different vent size was performed. The chosen vent diameters are 1cm and 2cm which corresponds to 4% and 8% of the total suction anchor diameter respectively. It was observed that for the same lowering velocity, the upward force due to air pressure increases with smaller vent size. Thus for the selected suction anchor model, it is inferred that the 2cm vent size is considered safe for lowering up to an average lowering speed of 1.5mm/sec.



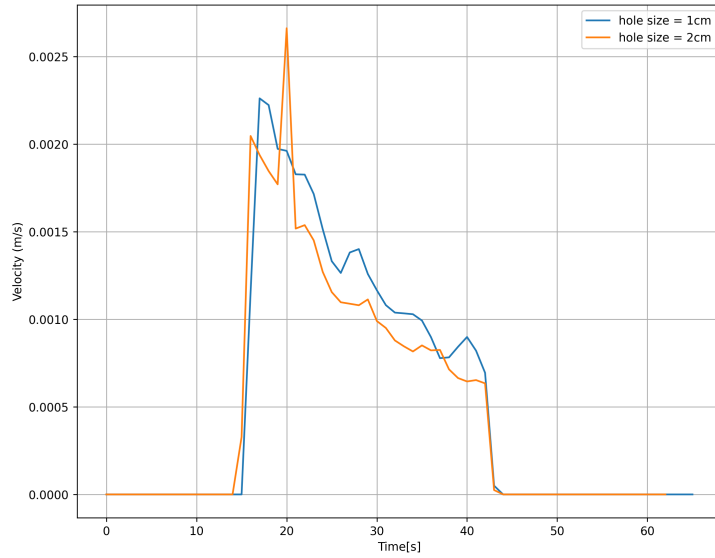


Figure 4.6: Velocity comparison for different vent valve size

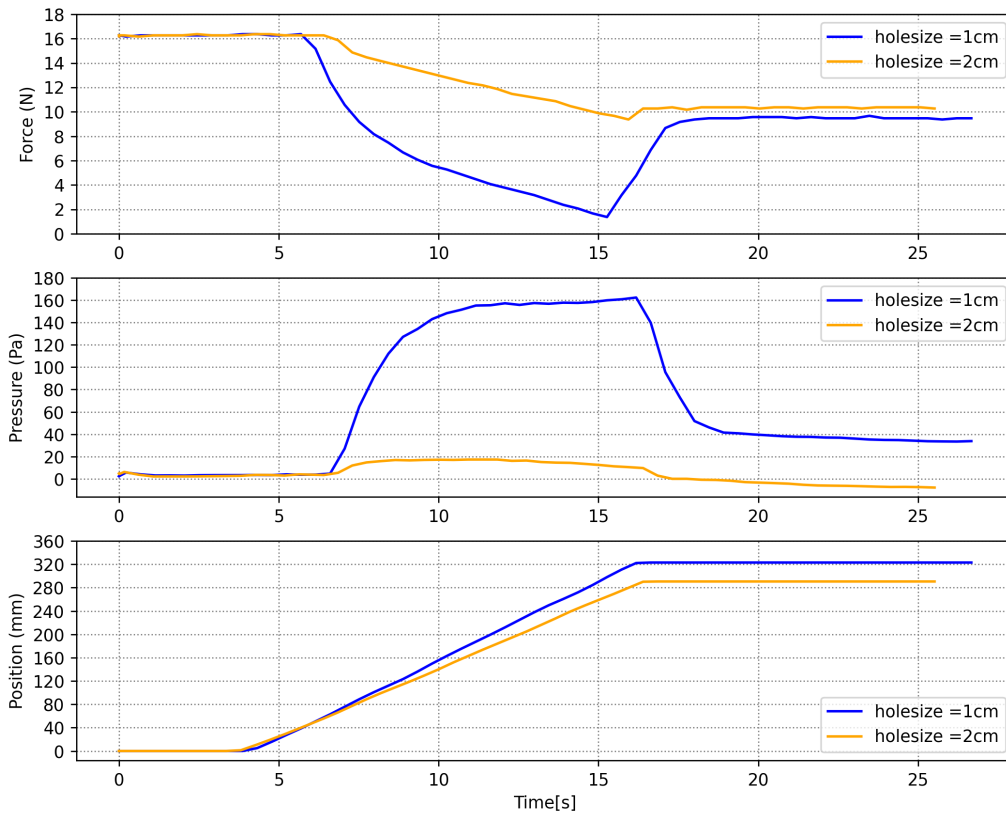


Figure 4.7: Varying vent valve size

# Chapter 5

## Discussion and Conclusion

The goal of this thesis was to investigate the influence of entrapped air effect as well as hydrodynamic effects during a suction anchor installation. To investigate these effects, scaled down experiments and numerical analysis was conducted. The scaled down experiments were chosen because full scale experiments were expensive.

To perform the experiments, the parameters that could influence the lowering process such as the pressure inside the suction anchor, its position and force acting on the lifting wire, were identified and an experimental setup was designed and developed to measure these parameters. The experimental setup consist of several electronic sensors, micro controllers and mechanical devices. This setup helped to replicate a scaled down version of suction anchor lowering procedure using crane. Additionally, it allowed for the integrated and synchronous measurement of data through out the lowering process. The scaled down experiments were conducted with a series of test cases that isolate each physical effects. These test cases were dry static, dry dynamic, wet closed static, wet closed dynamic and finally wet open dynamic case which represents the complete lowering process. Simultaneously, an analytical model was formulated and developed for each of these test cases. The analytical model which is an ordinary differential equation, was simulated using python ODE solver and the results were extracted. The experimental results were used to calibrate the mathematical model.

The static results of the numerical model produced good agreement with the experimental measurement. For the wet closed dynamic case, the modelled force and pressure had a good matched with the experiment data. There was a slight variation in the position and velocity data obtained. The reason for this mismatch could be that the mathematical model was not tuned correctly to represent the actual lowering process or an error in the position measured from the rotation sensor. Repeated experiments or more fine tuning of the mathematical model should have eliminated this variation. But this was not able to perform due to the time constraint. The experimental data for wet open dynamic case was compared with the mathematical model results. It was observed that looking at the value axis, the final pressure and force values from the simulation were matching with maximum pressure and minimum force values obtained from the experiment. There was a mismatch observed in the transient phase of the force and pressure curve. From the experimental data, there is an increase in pressure in the initial phase and then the pressure drops as the lowering velocity is decreased. There was a gradual decrease of pressure observed during lowering until it is stopped. The pressure inside the suction anchor was found to be a function

of both the lowering velocity and the vent hole size. When the suction anchor gets lowered into water, there is an increase of pressure due to the decrease in air volume. Also at the same time, there is a decrease in pressure due to the ventilation of air through the vent hole resulting in a coupled effect dependent on the lowering position, velocity and vent hole size. This could be the reason for the gradual decrease in the experimental pressure measurement until the lowering stopped. But this was not achieved in the simulation results and a clear mismatch was observed. The mathematical model predicts the net pressure inside the suction anchor as the sum of static pressure at that water depth and the pressure drop which was calculated using the pressure drop equation for orifice flow. The possible reason for the mismatch could be that the simulation model failed to capture the aforementioned coupling effect in the calculation of the inside pressure. To correct this error, the mathematical model should be extended or improved with coupled differential equation for the dynamic air pressure inside the suction anchor that well captures this gradual pressure decrease. Also, it was observed that there was a decrease in pressure after the lowering is stopped. This could be due to the ventilation of air through the valve until the pressure in and out of the suction anchor is equal.

For the full scale operations, what is more important is either to lower the suction anchor slowly or to increase the vent valve size to have a safe operation. However we do not have clear rules on how the lowering velocity and vent valve size influence the behaviour of the suction anchor. Therefore, a parametric study for evaluating the influence of lowering velocity and hole size on the net force acting on suction anchor was conducted using the developed experimental setup. The findings from the parametric study will be beneficial to evaluate whether the lowering velocity or the hole size has a better influence on the suction anchor behavior. Thus experiments were conducted for different lowering velocities with constant vent valve size. Moreover, experiments were conducted for different vent valve size making the lowering velocity same. From these experiments it was reasonable to conclude that for the selected suction anchor with D/H ratio of 0.83, a vent valve size of 2cm and a lowering velocity up to 1.5 mm/sec was considered safe. Additionally, from the obtained parametric study measurements, it was observed that there were considerable pressure increase during lowering at different velocities with smaller vent valve size. If the vent valve size has to be small, then to lower the suction anchor safely, the lowering velocity should be very low (0.6 mm/sec). In contrary for a medium lowering velocity (2mm/sec), the pressure curve did not even rise with an increased valve size. This showed that vent valve size has more influence on the lifting line force compared to the lowering velocity.

Since the study uses model scale, then it makes sense to run the analytical model in the same scale so as to avoid the scale problems. To relate these findings to full scale, proper scaling methods should be employed. For the friction force inside the suction anchor and the friction through vent valve, Reynolds's scaling will be appropriate method. To account for waves or hydrodynamic effects, the Froude scaling will be suitable. Furthermore, if it is slamming force that is focused, then there might be other scaling effects.

During a suction anchor lowering slamming occurs twice. First slamming occurs when the suction anchor bottom touches the water surface. The first entry does not create much severe slamming force on the suction anchor because the rigid surface is just a ring which is rather small. However, if it was a closed top, there could be some considerable slamming effect. But there is air inside the anchor which is a bit compressible as well as the ventilation of air together will reduce this slamming effect. After the occurrence of the first entry into water, the next slamming occurs when the suction anchor top impacts the water surface. It can be regarded as a "secondary

slamming" which can be related to the hydraulic shock that occurs in pipe flow of incompressible liquid when the flow hits the dead end. This is a classic problem in a hydraulic pipe flow but the focus for this study was on the first entrance slamming.

The findings from the above described results allow to address the thesis objectives raised in the beginning of this study. In the following each objective with the according findings and contributions are summarized.

1. "*How to conduct the experimental study on the entrapped air effect and hydrodynamic effects during suction anchor lowering?*" : An experimental setup consisting of electronic sensors, micro-controllers and mechanical devices was designed and developed to conduct scaled down experiments to study the entrapped air effect as well as hydrodynamic effect during suction anchor lowering.
2. "*How to analyse the lowering process numerically and validate it ?*" - A mathematical model for the suction anchor lowering process was developed and simulated. The experiments were conducted for different test cases that isolates each physical effect and its results were used to validate the simulation results of the mathematical model. However, some variations were observed and possible reasons for the deviation and ways to eliminate the errors were discussed.
3. "*Discuss ways to improve the suction anchor lowering process*" : The parameters such as lowering velocity and vent valve size that influences the behaviour of suction anchor while lowering into water was identified and a parametric study was conducted to find the optimum way to lower the suction anchor. The parametric study results were also used identify whether it is the vent valve size or the lowering velocity that has a better influence in the suction anchor behaviour. From the results it was observed that the vent valve size seemed to have a better influence than the lowering velocity.

# Chapter 6

## Future Works

The recommendations for future study are as follows:

1. The developed mathematical model could not capture the suction anchor behaviour in the transient phase. The model could be extended to have a more accurate calculation of the net pressure inside the anchor so that a better match with the experiment results is achieved.
2. For this study the scaled down experiments were conducted in still water. It would be interesting to conduct the experiments in waves to study the behaviour of the suction anchor during splash zone crossing. To perform this investigation, the developed experimental setup can be used to measure motion, force and pressure data throughout the lowering process. Additionally, the mathematical model could be extended to include the wave effects on the dynamic pressure inside the suction anchor.
3. For this study, the focus was only on the vertical motion of the suction anchor. The towing tank at NTNU Ålesund has installed camera assisted motion tracking system. If this system is integrated with the developed experimental setup, a more precise motion measurement of the suction anchor for all degrees of freedom can be achieved. This can give more detailed information on the behavior of suction anchor during lowering.
4. A parametric study with different top plate geometries will be beneficial to investigate its influence on the slamming force. The findings can be beneficial to have an optimum suction anchor design with reduced slamming forces.

# Bibliography

- [1] DET NORSKE VERITAS AS. “Modelling and analysis of marine operations”. In: *Recommended Practice: DNV-RP-H103* (2011).
- [2] Odd Faltinsen. *Sea loads on ships and offshore structures*. Vol. 1. Cambridge university press, 1993.
- [3] HX710B pressure sensor module-Pressure Sensor MPS20N0040D-S - Datasheet, ADC datasheet. [https://softroboticstoolkit.com/files/sorotoolkit/files/mps20n0040d-s\\_datasheet.pdf](https://softroboticstoolkit.com/files/sorotoolkit/files/mps20n0040d-s_datasheet.pdf),[https://win.adrirobot.it/datasheet/integrati/pdf/HX710\\_A-B.PDF](https://win.adrirobot.it/datasheet/integrati/pdf/HX710_A-B.PDF).
- [4] Manufatcurer- AMS-AS5600 rotation sensor - Datasheet. [https://ams.com/documents/20143/36005/AS5600\\_DS000365\\_5-00.pdf](https://ams.com/documents/20143/36005/AS5600_DS000365_5-00.pdf).
- [5] Manufatcurer- HBM-HBM S2M 1000N force sensor - Datasheet. <https://www.hbm.com/fileadmin/mediapool/hbmdoc/technical/B03594.pdf>.
- [6] Frøydis Solaas and Peter Christian Sandvik. “Hydrodynamic coefficients for suction anchors during installation operations”. In: *International Conference on Offshore Mechanics and Arctic Engineering*. Vol. 57779. American Society of Mechanical Engineers. 2017, V009T12A031.
- [7] Peter Stephan and VDI Heat Atlas. “B1 Fundamentals of Heat Transfer”. In: *VDI Heat Atlas* (2010), pp. 15–30.
- [8] Lixin Zhu and Hee-Chang Lim. “Hydrodynamic characteristics of a separated heave plate mounted at a vertical circular cylinder”. In: *Ocean Engineering* 131 (2017), pp. 213–223.

# Appendix A

## Simulation Code

```
1 import numpy as np
2 from scipy.integrate import solve_ivp
3 import matplotlib.pyplot as plt
4 import math
5 import pandas as pd
6 from matplotlib import dates
7 from matplotlib.ticker import MultipleLocator, ScalarFormatter
8
9 def suction_anchor_motion(t, y, m, rho, g, A, waterdepth, length, P_e, params, dia_hole):
10     # Define the ODE describing the suction anchor motion
11     dydt = y[1]
12
13     if y[0] > waterdepth:
14         depth = y[0]-waterdepth # Find the depth of the suction anchor
15         """
16         Quadratic solution steps to find inner water depth
17         """
18         a2 = 1
19         b= -(depth+length+(P_e/(rho*g)))
20         c = depth*length
21         h = (-b - np.sqrt((b**2)-(4*a2*c)))/(2*a2) # Determined the inner water depth
22
23         p_hydr = (depth-h)*rho*g
24         v_2 = C*np.sqrt((2*p_hydr)/rho_air)
25
26         p_vent = ((rho_air/2)*((v_2-dydt)**2))
27
28     #     print(f"v2 ={v_2}, v1 = {y[1]}")
29     if dia_hole==0:
30         p2 = p_hydr
31     else:
32         p2 = p_hydr - p_vent # presure inside the suction anchor
33
34     Amass = (2.09*rho*((dia/2)**3)) # Approximated added mass of a hemisphere with same cross se
35
```

```

36     fb = depth*(A-0.0459)*rho*g # underwater volume
37
38     dvdt = ((m * g)-fb-5 - (p2*A)-(mu*m*g*y[1]))/(m+(A*mass))
39
40     f = ((m) * g)-5 - (p2*A) )
41     else:
42         dvdt = ((m * g) -(mu*m*g*y[1]))/m
43         f = m * g
44         p2 = 0
45         p_hydr = 0
46         p_vent = 0
47
48
49     params.append([t,p2,f]) # Params : [time,pressure, net force]
50
51     return [dydt, dvdt]
52
53 # Define system parameters
54 m = 1.6 # Mass of the suction anchor (kg)
55 rho = 1000 # Density of water (kg/m^3)
56 rho_air = 1.28 #Density of air (kg/m^3)
57 g = 9.81 # Acceleration due to gravity (m/s^2)
58 dia = 0.25
59 dia_hole =0.002
60
61 beta = dia_hole/dia
62 C = 0.61/(np.sqrt(1-(beta**4)) )
63
64 A = (math.pi /4)*(dia**2) # Cross-sectional area of the suction anchor (m^2)
65 A_hole = (math.pi /4)*(dia_hole**2)
66 mu =15# Friction coefficient
67 P_e = 101325
68
69
70 waterdepth = 0.25# Water Depth
71 length = 0.3
72
73
74
75 # Define initial conditions
76 y0 = [0, 0] # Initial position and velocity of the suction anchor
77
78 # Define time span
79 t_span = [0, 25] # Start and end time of the simulation
80 num_points = 500
81 t_eval = np.linspace(t_span[0], t_span[1], num_points) # Time points for evaluating the solution
82 params = []
83
84 # Solve the ODE numerically
85 sol = solve_ivp(suction_anchor_motion, t_span, y0, args=(m, rho, g, A,waterdepth,length,P_e,params,

```



```

86
87 # Extract the solution
88 t = sol.t
89 disp_sim = sol.y[0]
90 vel_sim = sol.y[1]
91 params = np.array(params)
92
93 sim_df = pd.DataFrame()
94 sim_df['time'] = t
95 sim_df['position'] = disp_sim
96 sim_df['velocity'] = vel_sim
97
98 sim1_df = pd.DataFrame()
99 sim1_df['time'] = params[:,0]
100 sim1_df['pressure'] = params[:,1]
101 sim1_df['force'] = params[:,2]
102
103
104 """
105 Experimental data processing and comparison
106 """
107 import numpy as np
108 import matplotlib.pyplot as plt
109 from datetime import datetime
110 import pandas as pd
111 from matplotlib import dates
112 import matplotlib.axis as axs
113 from matplotlib.ticker import MultipleLocator, ScalarFormatter
114
115 seclocator = dates.SecondLocator(interval=2)
116 minlocator = dates.MinuteLocator(interval=1)
117
118 def Velocity(displacement, time):
119     velocity = []
120     for i in range(1, len(displacement)):
121         dt = time[i]
122         vel = (displacement[i] - displacement[i - 1]) / dt
123         velocity.append(vel)
124     return velocity
125
126 def centered_moving_average(data_in, win):
127     n = len(data_in)
128     data_out = np.zeros(n-win)
129     for i in range(0, n-win):
130         if i < win :
131             seg = data_in[:win]
132             seg_mean = np.mean(seg)
133             data_out[i] = seg_mean
134         elif i > win & i < n-win:
135             seg = data_in[i-(win//2): i+(win//2)]

```

```

136         seg_mean = np.mean(seg)
137         data_out[i] = seg_mean
138     else:
139         seg = data_in[n-win:]
140         seg_mean = np.mean(seg)
141         data_out[i] = seg_mean
142     return data_out
143
144 disp = []
145 pressure1 = []
146 force = []
147 time_list = []
148 with open(r"data.dat") as f:
149
150     for line in f:
151         try:
152
153             time = f.readline().split(',')[0]
154             time_list.append(time)
155             d = f.readline().split(',')[1]
156             d = float(d[1:])
157             disp.append(d)
158             p = float(f.readline().split(',')[2])
159             pressure1.append(p)
160             forc = float(f.readline().split(',')[3][:-2])
161             force.append(forc)
162         except:
163             continue
164
165 time_list = [datetime.strptime(a, "%Y-%m-%d_%H:%M:%S.%f") for a in time_list]
166 time_list = time_list[79:]
167 initial_time = time_list[0]
168 time_list = [i - initial_time for i in time_list]
169 timestamp = [i.total_seconds() for i in time_list]
170
171 vel_exp = Velocity(disp[79:], timestamp)
172
173
174 # exp_df = pd.DataFrame({'time': timestamp, 'pressure': pressure1 })
175 exp_df = pd.DataFrame()
176 exp_df['time'] = pd.Series(timestamp)
177 exp_df['position'] = pd.Series(disp[79:])
178 exp_df['force'] = pd.Series(force[79:])
179 exp_df['velocity'] = pd.Series(vel_exp)
180 exp_df['pressure'] = pd.Series(pressure1[79:])
181 exp_df = exp_df.dropna(axis=0)
182
183 import matplotlib.axis as axis
184 from matplotlib.ticker import MultipleLocator, ScalarFormatter
185

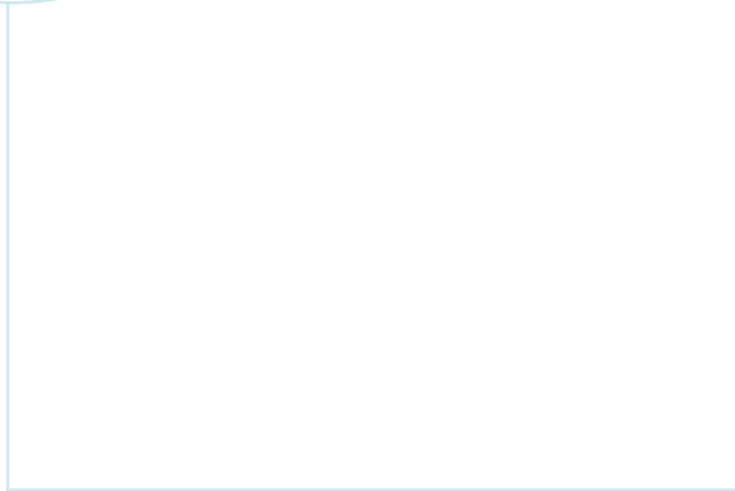
```

```

186 # seclocator = dates.SecondLocator(interval=1)
187 # minlocator = dates.MinuteLocator(interval=1)
188
189 fig = plt.figure(figsize=(10,6),dpi=500, facecolor='w',edgecolor='k')
190
191
192
193
194 ax1 = fig.add_subplot(4,1,1)
195 ax1.plot(exp_df['time'],exp_df['force']+15.57,label='Experiment')
196 ax1.plot(sim1_df['time'],sim1_df['force'],label="Simulation",color='r')
197 ax1.set_ylabel('Force_(N)')
198 ax1.legend()
199
200 ax1.grid()
201
202 ax2 = fig.add_subplot(4,1,2)
203 ax2.plot(exp_df['time'],exp_df['pressure'],color='g',label="Experiment")
204 ax2.plot(sim1_df['time'],sim1_df['pressure'],label="Simulation")
205 ax2.set_ylabel('Pressure(Pa)')
206 ax2.legend(loc= 'upper_right')
207
208 ax2.grid()
209 ax3 = fig.add_subplot(4,1,3)
210 ax3.plot(sim_df['time'],sim_df['position']*1000,label="Simulation")
211 ax3.plot(exp_df['time'],exp_df['position'],label="Experiment")
212 ax3.set_ylabel('Position_(mm)')
213 ax3.legend(loc= 'upper_right')
214
215
216 ax3.grid()
217 plt.text(0.1, 2.5, 'Water_contact', transform=ax3.transAxes,fontsize=9)
218 plt.text(0.02, 2.5, 'Lowering_\nstarted', transform=ax3.transAxes,fontsize=9)
219 plt.text(0.45, 3, 'Lowering_\nstopped', transform=ax3.transAxes,fontsize=9)
220
221 ax4 = fig.add_subplot(4,1,4)
222 ax4.plot(exp_df['time'],exp_df['velocity'],label="Experiment")
223 ax4.plot(sim_df['time'][1:],sim_df['velocity'][1:]*1000,label="Simulation")
224 ax4.set_ylabel('velocity_(mm/sec)')
225 ax4.legend()
226 ax4.grid()
227
228 plt.xlabel('Time_[s]')
229
230 ax1.axvline(exp_df['time'][0],linewidth=1.5,color='r',alpha=0.8,ls='--')
231 ax2.axvline(exp_df['time'][0],linewidth=1.5,color='r',alpha=0.8,ls='--')
232 ax3.axvline(exp_df['time'][0],linewidth=1.5,color='r',alpha=0.8,ls='--')
233 ax4.axvline(exp_df['time'][0],linewidth=1.5,color='r',alpha=0.8,ls='--')
234
235 ax1.axvline(exp_df['time'][5],linewidth=1.5,color='r',alpha=0.8,ls='--')

```

```
236 ax2.axvline(exp_df['time'][5],linewidth=1.5,color='r',alpha=0.8,ls='--')
237 ax3.axvline(exp_df['time'][5],linewidth=1.5,color='r',alpha=0.8,ls='--')
238 ax4.axvline(exp_df['time'][5],linewidth=1.5,color='r',alpha=0.8,ls='--')
239
240 ax1.axvline(exp_df['time'][28],linewidth=1.5,color='r',alpha=0.8,ls='--')
241 ax2.axvline(exp_df['time'][28],linewidth=1.5,color='r',alpha=0.8,ls='--')
242 ax3.axvline(exp_df['time'][28],linewidth=1.5,color='r',alpha=0.8,ls='--')
243 ax4.axvline(exp_df['time'][28],linewidth=1.5,color='r',alpha=0.8,ls='--')
244
245
246
247 fig.savefig("DynamicWetClosedExp")
248
249 plt.show()
```



 **NTNU**

Norwegian University of  
Science and Technology